REVIEW

Engineering current collectors for advanced alkali metal anodes: A review and perspective

Liang Hu[1] | **Jiaojiao Deng[2]** | **Qinghua Liang[3]** | **Junxiong Wu[4]** | **Bingcheng Ge[1]** | **Qiang Liu[1]** | **Guohua Chen[1]** | **Xiaoliang Yu[1]**

[1]Department of Mechanical Engineering, Research Institute for Smart Energy, The Hong Kong Polytechnic University, Hung Hom, Hong Kong, China

[2]Shenzhen Key Laboratory on Power Battery Safety and Shenzhen Geim Graphene Center, Tsinghua Shenzhen International Graduate School (SIGS), Shenzhen, China

[3]Department of Chemical Engineering, The University of Melbourne, Parkville, Victoria, Australia

[4]College of Environmental and Resource Sciences and College of Carbon Neutral Modern Industry, Fujian Normal University, Fuzhou, China

Correspondence

Guohua Chen and Xiaoliang Yu, Department of Mechanical Engineering, Research Institute for Smart Energy, The Hong Kong Polytechnic University, Hong Kong, China.
Email: xiaoliang.yu@polyu.edu.hk and guohua.chen@polyu.edu.hk

Abstract

Alkali metal batteries (AMBs) are promising next-generation high-density electrochemical energy storage systems. In addition, current collectors play important roles in enhancing their electrochemical performances. Thus, it is essential to have a critical review of the most recent advances in engineering the current collectors for high-performance AMBs. In this review paper, the fundamentals of alkali metal deposition on current collectors will be introduced first. Then recent advances in the development of advanced metal and carbon-based current collectors are examined for boosting the stability and cycle life of lithium metal batteries (LMBs) in terms of various strategies including 3D architectural design and functional modifications. Thereafter, the research progress in design of advanced current collectors will be analyzed for sodium/potassium metal batteries, especially the counterparts that do not follow the paradigms established in LMBs. Finally, the major challenges and key perspectives will be discussed for the future development of current collectors in AMBs.

KEYWORDS

alkali metal batteries, carbonaceous, current collector, functional modification, metallic, three dimensional

1 | INTRODUCTION

Li-ion batteries (LIBs) have predominated the global market of electrochemical energy storage (EES) over the past decades, especially in electric vehicles and portable electronic devices.[1,2] However, the available intercalation-based electrodes in LIBs can only offer an maximum energy density of $\sim$300 Wh kg^{-1}, a value that cannot meet the ever-increasing demand for high-density EES systems.[3] Alkali metals have attracted extensive research attention as

promising alternative anodes for the next-generation battery technologies. They own ultrahigh theoretical capacities of 3860, 1166, and 685 mAh g^{-1} and low redox potentials of -3.040, -2.714, and -2.930 V vs. standard hydrogen electrode (SHE) for Li, Na, and K, respectively.[4] Despite the inferior electrochemical potential and specific capacity of Na and K to those of Li, the natural abundance, wide distribution, and low cost of Na and K resources make them great promising anodes for large-scale energy storage.[5,6]

Currently, the practical applications of alkali metal batteries (AMBs) are still hindered by their short cycle lives and severe safety issue. Alkali metals are highly reactive with the components in liquid electrolytes and would form solid electrolyte interphase (SEI) on the metal anode surface.[7] Owing to the large volume fluctuation during alkali metal plating/stripping, the SEI layer tends to break and expose the inner fresh metal. This will result in the low Coulombic efficiency and poor cycling stability of AMBs because of the continued consumption of the electrolyte components.[8] Moreover, the plating/stripping of alkali metal on planar current collectors is normally ununiform and would lead to dendrite growth, especially at high current rates. The dendrites may penetrate the separator to result in short circuit between the cathode and anode, causing fires or even explosions.[9]

To extend the lifespan and address the safety concern of AMBs, a variety of approaches including traditional "trail-and-error" processes, computational chemistry, high-throughput screening, and machine learning have been developed.[10] Novel electrolytes have been developed to better accommodate the hyper-reactive alkali metals[4,10,11]; separator modifications have been performed to improve the mechanical strength and alter the interface compatibility between metallic anodes and electrolytes[12]; artificial SEI layers have been fabricated for better homogeneity of component distribution and mechanical robustness[13–15]; and advanced metallic anode architectures have been constructed to accommodate the volume fluctuation during charge/discharge and to suppress the dendrite growth.[16,17] For a typical battery system, the rational choice of electrode current collector is a precondition for its successful operation. Although alkali metals have considerable electron conductivity, using alkali-metal anode without the current collector remains a great challenge. Generally, the high surface roughness of alkali metal foil is unfavorable for uniform metal deposition. The electronic conductivity of alkali metal anodes would gradually decrease over redox cycling due to the continuous growth of SEI. In recent years, more research attention has been paid to the design of advanced current collectors toward the inhabitation of the dendrites growth of alkali metal and the regulation on the redox cycling behavior in AMBs. For instance, utilizing a high-surface-area current collector (i.e., 3D or porous metallic and carbonaceous current collectors) could decrease the local current density along the anode surface.[18–21] Coating lithiophilic modification layer could bring down the energy barrier for alkali metal nucleation and facilitate uniform metal plating.[22–24]

In view of the recent increase in research activity involving current collector engineering for AMBs, a timely and comprehensive review is necessary to investigate this intriguing and continuously developing field of research. This work goes beyond existing research progress reports on current collector design for rechargeable batteries.[25,26] Novel measures/technologies proposed recently, current collector design for various alkali metal batteries, as well as a systematic classification, are demonstrated to better reflect the advancement of this research area.

In this review, the fundamentals of alkali metal deposition on current collectors of AMBs will be introduced first. The recent research progress on metallic and carbonaceous current collectors in lithium metal batteries (LMBs) will be examined in terms of various strategies such as the 3D architectural design and functional modifications with a special focus on the structure-composition-performance relationship (Figure 1). Thereafter, the recent design of advanced current collectors is analyzed for sodium/potassium metal batteries. In particular, the advances reported for Na and K counterparts that do not follow the paradigms established in LMBs will be discussed. Finally, the remaining challenges and key perspectives will be presented in engineering the current collectors, hoping to inspire the development of novel current collectors for practical applications of AMBs.

2 | FUNDAMENTALS ON ALKALI METAL DEPOSITION: FROM NUCLEATION TO EARLY GROWTH

The extensive research efforts have been made on inhibiting alkali metal dendrite growth and extending the lifespan of AMBs. Morphological evolution and overall performance of alkali metal anodes are the major focuses of research. Mitigating or eliminating alkali metal dendrites at the source is of similar significance. Alkali metal deposition occurs when alkali metal ions migrate and receive electrons from a current collector. The subsequent deposition takes place preferentially along with the initial formation of nuclei.[34] Thus, alkali metal nucleation and early growth behavior play a critical role in determining the final deposition morphology. Extensive research efforts have been devoted to investigating the mechanism and various models have been established.[35–38] Among
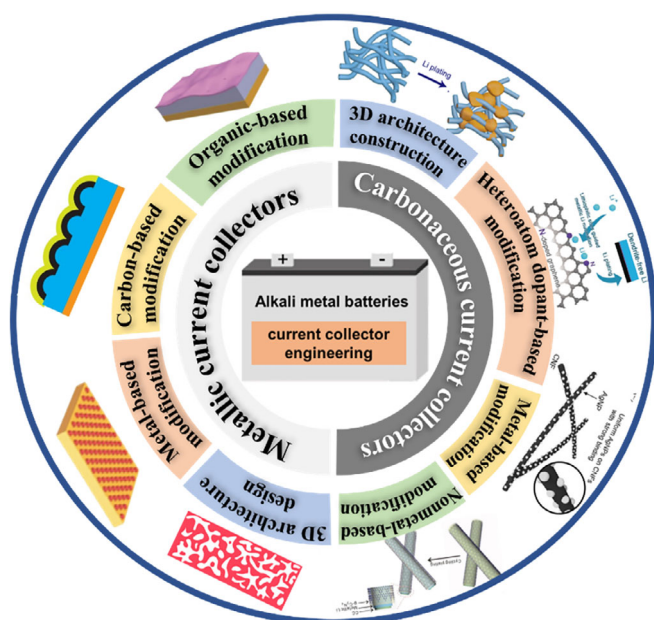
FIGURE 1 The strategies of engineering current collectors for advanced dendrite-free alkali metal batteries: 3D architecture design. Reproduced with permission: Copyright 2018, Elsevier.[20] and Copyright 2017, Elsevier.[27] Metal-based modifications. Reproduced with permission: Copyright 2017, John Wiley & Sons, Inc.[28] and Copyright 2017, John Wiley & Sons, Inc.[29] Carbon-based modification on metallic current collector. Reproduced with permission: Copyright 2014, Springer Nature.[30] Organic-based modification on metallic current collector. Reproduced with permission: Copyright 2016, John Wiley & Sons, Inc.[31] Heteroatom dopant-based modification on carbonaceous current collector. Reproduced with permission: Copyright 2017, John Wiley & Sons, Inc.[32] Nonmetal-based modification on carbonaceous current collector. Reproduced with permission: Copyright 2019, John Wiley & Sons, Inc.[33]

them, the heterogeneous model[37] and the space charge model[38] are the two most accepted to describe the nucleation and early growth process. Some other models, including the surface diffusion model,[28,39] SEI-induced nucleating model,[40–42] and crystallography model[43,44] are also reported and will be briefly discussed in this section. Note that in these models Li metal is particularly exemplified to analyze the mechanism for alkali metal nucleation and growth.

2.1 | Heterogeneous model

Alkali metals and the current collector are intrinsically heterogeneous. Therefore, deep understanding and controlled regulation of heterogeneous nucleation are of great significance in AMB study.

Heterogeneous nucleation was first studied by Ely and Gacia.[37] Thermodynamic and kinetic analyses were performed via theoretical simulation to forecast the

initial Li nucleation and early growth upon heterogeneous electrodeposition in the reaction-rate-limited systems. As shown in Figure 2A, the heterogeneous nucleation and growth behaviors include five regimes: nucleation suppression, long incubation time, short incubation time, early growth, and late growth. In the nucleation suppression regime, nucleation embryos are thermodynamically unstable and inevitably redissolve into the electrolyte. By contrast, the embryos in the long incubation time regime are metastable. Those thermodynamically favorable ones keep stable without any pronounced growth until the thermal fluctuations make metal growth kinetically favorable. As the overpotential surpasses the critical value, the short incubation time regime gives rise to the formation of embryos with narrow size distributions. The deposited alkali metal embryos with a critical thermodynamic radius rapidly nucleate and grow. In the early growth regime, the thermodynamically and kinetically stable nuclei continuously grow to reach a constant growth rate. Finally, in the late growth regime, the morphology and microstructure of deposits are predominated by the externally localized electric fields.

Based on the above analysis of the heterogeneous model, several measures can be taken to inhibit dendrite growth. First, decreasing the roughness of the electrode surface to extend the incubation time. Second, regulating the overpotential of alkali metal nucleation below the critical value to facilitate uniform nucleation. For instance, improving the affinity of current collectors with alkali metal species via coating with lithiophilic layer. Third, controlling the particle size of metal deposits below the critical thermodynamic radius to retard dendrite growth.

2.2 | Space charge model

Chazalviel developed a space charge theory to clarify the lithium nucleation and growth behavior.[38] In this model, a battery cell utilizing a binary electrolyte was polarized at a constant current rate (Figure 2B). The distinct electrochemical behaviors were simulated and forecast for the anionic and cationic concentrations. When the anionic concentration drops to zero at Sand's time, the cationic concentration declines to a small yet positive value, leading to excessive positive charges at the anode surface. A localized space charge was thus generated along with a large electric field. Consequently, a serious deterioration of intrinsic instability of the system occurs and metal dendrites appear.

In space charge model, two distinctive regions are defined; Region I in bulk electrolyte and Region II on the surface of the electrode (Figure 2C). In Region II, there is
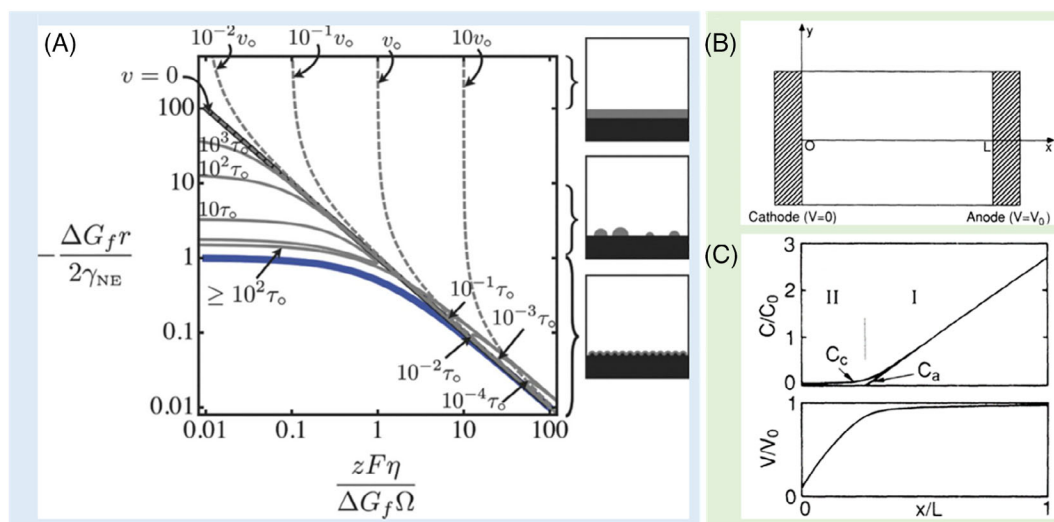
FIGURE 2 (A) Regimes of behavior during the initial stages of nucleation and growth: nucleation suppression (below the blue curve), long incubation time and short incubation time (above the blue curve and below the black curve), early growth and late growth (above the black curve). Reproduced with permission: Copyright 1990, American Physical Society.[37] (B) Scheme of the cell. (C) Profile of the ion concentrations and the electrostatic potential resulting from the numerical simulation in the hypothetical case of uniform deposition with negligible growth of the cathode. Reproduced with permission: Copyright 2013, IOP Publishing[38]

an ion-depleted area near the anode, where the potential declines and a space charge Z_ceC_0 is generated. According to this model, dendrite growth is initiated in Sand's time, when the concentration of cations drops to zero and the potential diverges. Rosso et al. calculated Sand's time via the following equation:

$$\tau_s = \pi(C_0eZ_c/2)^2(1+\mu_c/\mu_a)^2 \qquad (1)$$

where τ_s is the Sand's time, D is the diffusion coefficient of Li$^+$, C_0 is the original cationic concentration, Z_c is the valency of cations, J is effective electrode current density, μ_a and μ_c are the anionic and cationic mobilities, respectively.[45]

From this equation, it can be predicted that the following approaches may efficiently suppress the dendrite growth: (1) utilization of high concentration electrolytes, (2) electrolyte formulations with high lithium-ion transference number, and (3) the decrease of the local current density via 3D Li hosts. All these strategies have been verified to be effective experimentally.[46,47]

2.3 | Other models

2.3.1 | Surface diffusion model

The surface diffusion process plays a critical role in determining the alkali metal deposition behavior. Lowering the surface diffusion barrier and thus facilitating the surface migration is quite favorable for uniform metal deposition. For instance, the Li$_2$CO$_3$ component in SEI has

low surface energy but high diffusion barrier for Li-ions, easily generating dendritic growth.[39] In contrast, LiF has higher surface energy but a much lower surface diffusion barrier. Therefore, uniform deposition and dendrite-free morphology can be obtained.[28]

2.3.2 | SEI-induced nucleating model

SEI film is a crucial component at the Li metal surface. It is not stable and can be easily broken owing to the severe volume fluctuation upon Li plating/stripping. There are still arguments on the formation sequence of SEI and Li deposits.[40] Some researchers think that SEI is generated on the surface of Li metal anode immediately after Li nucleation. After that, the growth of Li deposits and even dendrites are modulated by ion diffusion through the SEI, where the diffusion barrier is higher than that of electrolytes. The fragile SEI breaks down because of the volume change derived from local stress, and then exposes and reacts with the electrolyte to form new SEI.[41] On the other hand, SEI formation was also reported to be ahead of Li nucleation by in-situ electrochemical transmission electron microscopy (TEM).[42]

2.3.3 | Crystallography model

Li plating on current collector surfaces involves the nucleation and subsequent growth of Li crystals. The

crystallographic orientation of Li metal can significantly affect the morphology of Li deposits. Li metal owns a body-centered cubic (BCC) crystal structure, and Li deposit grows favorably along the <111> direction.[44] Therefore, it tends to form single-crystalline Li metal nanowires. However, in a practical lithium metal battery cell, SEI is produced at the Li metal surface. This results in a much more complex growth process. In particular, under high external pressure, the favorable orientation of Li crystal would be disturbed, resulting in 2D Li metal growth.[43]

From the analyses based on the above models, it can be deduced that localized current density and surface chemistry are two crucial factors in current collector engineering toward regulated nucleation/growth. Therefore, in the following sections, we shall focus on the recent progress in 3D architectural design and functional modifications of current collectors. It is worth noting that many of the reported research works combine both the current density and surface chemistry factors for regulating alkali metal nucleation/growth.

3 | ADVANCED METALLIC CURRENT COLLECTORS FOR LITHIUM METAL ANODES

Planar metal foils, especially Cu foils, have been widely employed as the current collectors in LMBs because of their high electronic conductivity, good stability against Li metal, and good compatibility with the roll-to-roll process.[48] However, at a practical current density and areal capacity (4 mA cm^{-2}, 2 mA h cm^{-2}), the inhomogeneous Li-ion flux distribution on planar current collectors could cause non-uniform Li deposition and dendrite growth.[49] The utilization of 3D architectured current collectors with larger surface areas is an effective approach to reduce the local current density and thus promote the even distribution of Li$^+$ flux. Besides, modification of the current collector surface by functional materials is another efficient strategy to decrease the Li nucleation barrier and facilitate homogeneous nucleation.

3.1 | Nonplanar Cu current collectors for lithium metal anodes

In recent years, the design and fabrication of 3D multifunctional architectures in metal-based current collectors have attracted extensive research attention. Their high specific surface areas and large porosities can efficiently decrease the local current density, regulate the electric field distribution, and accommodate well the volume

fluctuation during Li plating/stripping.[50–53] There are generally two approaches to fabricate metal-based 3D current collectors, i.e., top-down approach and bottom-up approach. The former one involves the chemical/electrochemical corrosion of bulk metal into nanophases or porous architectures, while the latter one is meant by the preparation of metal nanophases (nanowires, nanoflakes) through chemical reactions among atoms, ions and molecules.

3.1.1 | Top-down fabrication

Dealloying is a facile way to produce pores in bulk metal materials, and commercial Cu–Zn alloy (brass) is the most common precursor to produce a 3D porous Cu current collector (Figure 3A). Tuan and co-workers synthesized nanoporous Cu films with different porosities, ligaments, and pore sizes through chemical dealloying of Cu–Zn alloy films.[54] The dissolution of Zn results in a bicontinuous microstructure of metal and voids. Then, Yun and co-workers fabricated a 3D porous Cu current collector by using a similar chemical dealloying of commercial brass.[51] It not only well accommodates the deposited Li metal but also effectively decreases the local current density by the large internal surface area. An electrochemical etching method was reported by Zhao and co-workers to remove the Zn component through a linear sweep voltammetry technique.[55] Compared with the chemical dealloying 3D Cu current collector, the electrochemically etched counterpart presents three times higher tensile strength of 13.5 MPa (Figure 3B). Moreover, the electrochemical dealloying process preserves the conductive network of Cu-Zn alloy well $(1.12 \times 10^5 \text{ S cm}^{-1})$, which is near an order of magnitude higher than $1.31 \times 10^4 \text{ S cm}^{-1}$ of the chemically dealloyed 3D Cu. The as-fabricated 3D Cu-based anode presents an average CE of 97.9% over 200 cycles at a current density of 1 mA cm^{-2} and an areal capacity of 1 mAh cm^{-2} (Figure 3C). Besides, An and co-workers reported a low–cost, eco–friendly vacuum distillation method for large-scale production of 3D current collectors.[20] Cu–Ga alloy was also reported in the production of a 3D porous Cu current collector by Shi and co-workers, which demonstrates three times the specific surface area of the brass counterpart.[56]

The above reported 3D Cu current collectors possess pore sizes on the scale of several micrometers, and the achieved areal capacity is generally less than 3 mAh cm^{-2}. Guo's group further investigated the morphology of deposited lithium on vertically aligned Cu microchannels with different pore radii, depths, and pore spacing.[52] The COMSOL Multiphysics simulation demonstrated

that the local current density in the microchannels is larger than that of the upper surface (Figure 3D). Therefore, Li is preferably nucleated inside the channels, and the porous Cu current collector with a larger surface area and appropriate pore volume exhibited better cycling and rate performance.
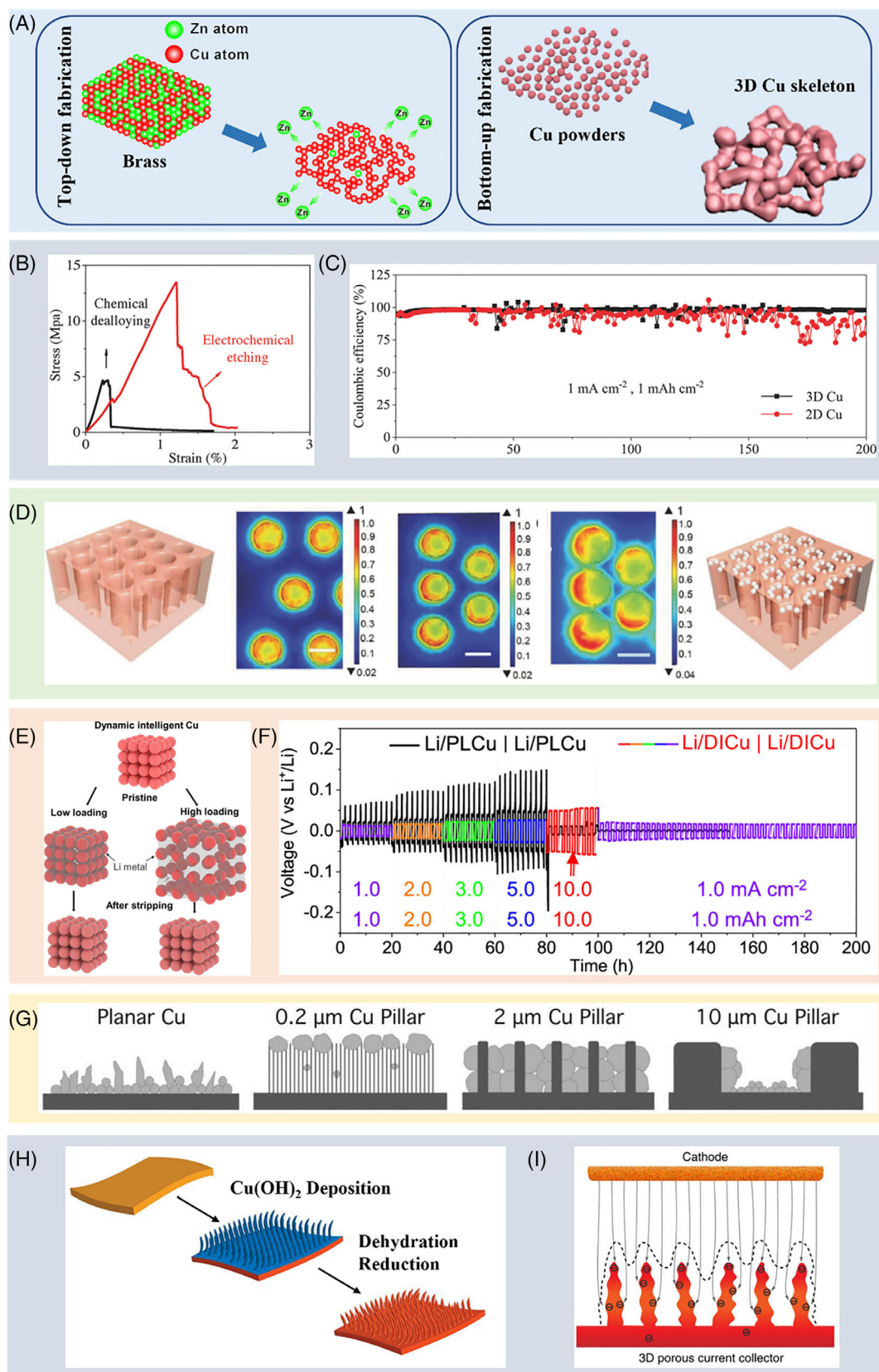

FIGURE 3 Legend on next page.

FIGURE 3 (A) Schematic illustration of top-down fabrication and bottom-up fabrication. (B) Stress–strain curves of 3D Cu current collectors fabricated by chemical dealloying method and electrochemical etching method. Reproduced with permission: Copyright 2018, Elsevier.[20] (C) Coulombic efficiencies of Li plating/stripping on 2D and 3D Cu current collectors under 1 mA cm^{-2} with a capacity of 1 mAh cm^{-2}. Reproduced with permission: Copyright 2018, John Wiley & Sons, Inc.[55] (D) Schematic diagram of the porous Cu current collectors and Li deposition on the porous Cu, and simulation results of the current density distribution on the surface of porous Cu with different pore spacings of 12, 16, and 20 μm. The numbers are ratio between the current density represented by one color and the maximum current density, the scale bars in the images are 10 μm. Reproduced with permission: Copyright 2017, John Wiley & Sons, Inc.[52] (E) Schematic illustration of dynamical changes of dynamic intelligent Cu current collector during Li plating/stripping. (F) Voltage verse time profiles of Li plating/stripping on dynamic intelligent Cu and the planar Cu electrodes at current densities of 1.0, 2.0, 3.0, 5.0, and 10.0 mA cm^{-2} for 1 h. Reproduced with permission: Copyright 2020, American Chemical Society.[57] (G) Schematic diagram of Li deposition on the planar Cu electrode, 0.2, 2, and 10 μm Cu pillars. Reproduced with permission: Copyright 2018, John Wiley & Sons, Inc.[58] (H) Schematic illustration of the 3D porous Cu foil fabrication. (I) Illustration of the Li deposition on a 3D current collector. Reproduced with permission: Copyright 2015, Springer Nature[50]

3.1.2 | Bottom-up fabrication

Constructing 3D Cu skeletons with appropriate nano-scale building blocks is a promising approach to produce advanced current collectors in LMBs.[48] Wang and co-workers reported NaCl-assisted powder-sintering of Cu powders to fabricate a 3D Cu skeleton with micrometer-sized open pores.[59] When employed as an anode for LMB, it showed an average CE of 95% over 700 cycles at 0.5 mA cm^{-2}. However, high-capacity lithium plating/stripping within the rigid 3D current collectors caused damage to the 3D structure, especially at high current rates. To address this issue, Chen and co-workers proposed a dynamic intelligent Cu skeleton that spontaneously adapts to the variation of volume by altering the packing density of the assembled Cu microparticles, enabling quick stress relaxation (Figure 3E).[57] To be specific, the voids among Cu microparticles can accommodate a certain amount of Li without causing an obvious volume expansion. After all the voids are filled, the interaction among Cu microparticles is changed, with Li metal working as a binder instead of the polyvinylidene difluoride (PVDF) polymer. As such, a 100 μm thick Cu microparticles-based film on Cu foil can be deposited with Li of a high capacity of 10 mAh cm^{-2}, and the dynamic Cu current collector maintains a small voltage hysteresis even after prolonged cycling at 10.0 mA cm^{-2} (Figure 3F). In contrast, the planar Cu electrode demonstrates a dendrite-induced failure under the same test conditions.

Besides Cu microparticles, Cu nanowires/nanofibers/nanopillars can also serve as the building blocks in the 3D scaffold. Yu's group reported an open porous and free-standing network constructed by Cu nanowires.[60] The high porosity enables a high Li deposition capacity of 7.5 mAh cm^{-2}. The as-fabricated lithium metal anode (LMA) achieved a low voltage hysteresis of ∼0.04 V over 200 cycles and show an average CE of ∼98.6%. Chen and co-workers fabricated vertically aligned Cu pillar arrays

by a templated electrodeposition method.[58] By adjusting geometric parameters including pillar diameter, spacing, and length, the nucleation density, average growth size and shape of deposits, and dead Li formation can be well controlled (Figure 3G). Cu pillar arrays with a 2 μm pillar diameter and an average pore spacing of 5 μm showed the optimized electrochemical performance. Besides, when compressed against the Cu pillars, the vertical pillar architecture can cause local deformation of separators. The Li-ion flux on top of the pillars was blocked, thus Li deposition is preferably to occur within the pores, minimizing the risk of hazardous short-circuiting.

Yang and co-workers fabricated a 3D Cu foil with a submicron skeleton by reduction of in-situ grown Cu(OH)$_2$ to Cu (Figure 3H).[50] The fabricated bunches of Cu fibers form a jungle-like porous layer, and the numerous nanosized protuberant tips on the surface function as the charge centers and nucleation sites (Figure 3I). With lithium metal accommodated in such a 3D current collector, the as-produced Li metal anode shows a low voltage hysteresis of <50 mV after cycling for 600 h.

3.2 | Metal-based modification

The lithiophobic nature of bare Cu foils makes them unsuitable as current collectors for loading lithium metal directly. The high nucleation barrier restricts the homogeneous lithium nucleation and accelerates the uncontrolled growth of mossy/dendritic lithium.[61] Introduction of alloying metals and metal compounds with excellent lithium affinity can effectively address this issue and prolong the lifespan of LMBs.

3.2.1 | Heterometal modification

Metal elements, such as Au, Ag, Sb, and Zn, can alloy with Li.[61] Therefore, modifying Cu foil with these
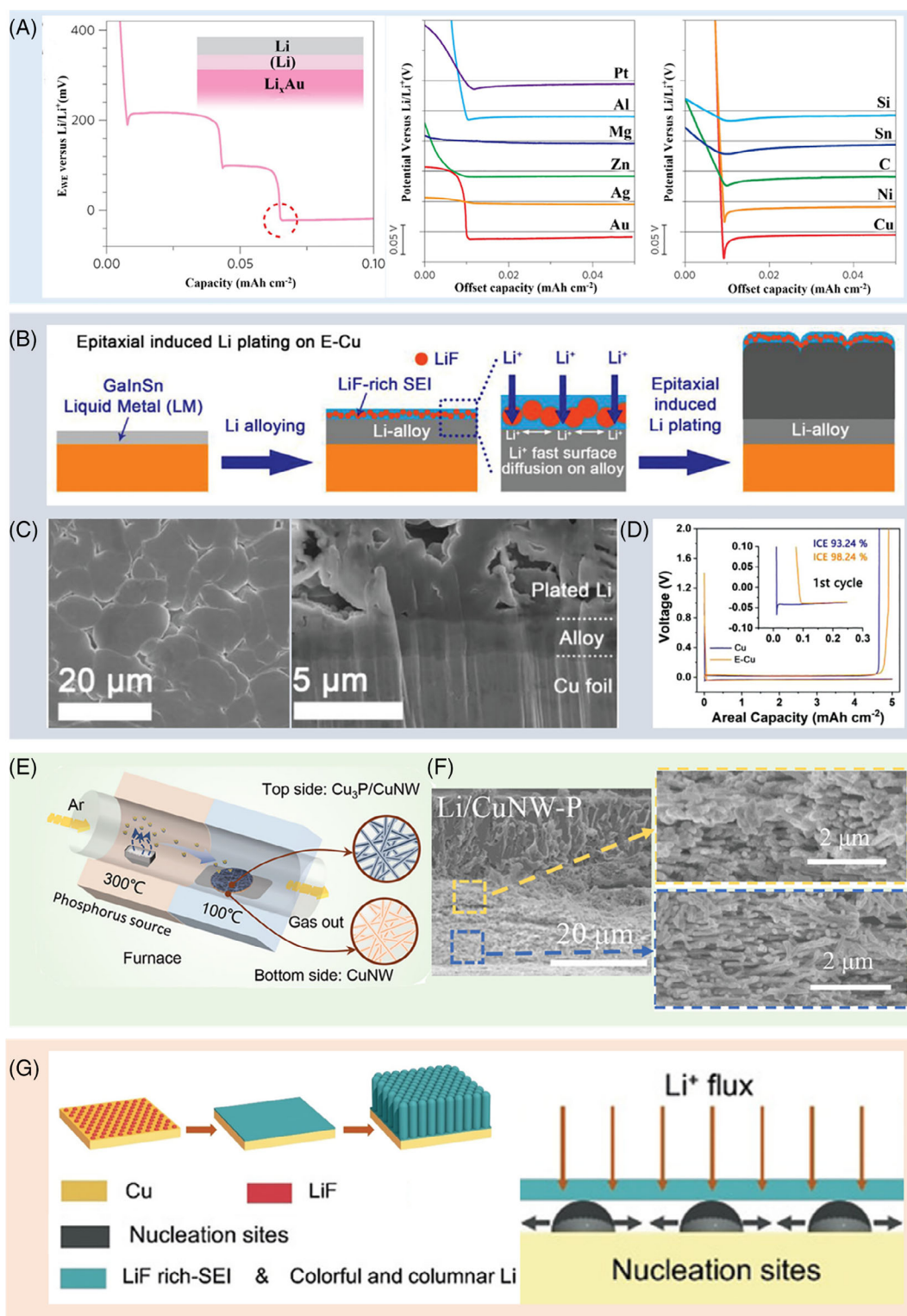
FIGURE 4 (A) Voltage profiles of galvanostatic Li deposition on a gold substrate and comparison of Li nucleation overpotential on various substrates. Reproduced with permission: Copyright 2016, Springer Nature.[61] (B) Schematic illustration of Li alloying and epitaxial induced plating behaviors on E-Cu. (C) Top view and cross-sectional SEM images of E-Cu current-collector after Li plating. (D) Voltage profiles of Cu/Li and E-Cu/Li asymmetric cells cycling with capacities of 5 mAh cm^{-2} under 0.5 mA cm^{-2}. Reproduced with permission: Copyright 2021, John Wiley & Sons, Inc.[65] (E) Schematic of the phosphidation reaction of Cu nanowires. (F) Cross-sectional SEM images of Li deposition on the copper nanowire-phosphide current collector. Reproduced with permission: Copyright 2019, John Wiley & Sons, Inc.[66] (G) Schematic diagram of the Li plating morphologies on LiF-modified Cu surface. Reproduced with permission: Copyright 2017, John Wiley & Sons, Inc.[28]

lithiophilic metals can effectively reduce the overpotential of lithium nucleation. Yan and co-workers found the overpotential barrier of the heterogeneous nucleation of Li on Cu substrate to be as high as 40 mV, because of the high degree of thermodynamic mismatch between Li and Cu.[61] Au not only forms an alloy with Li but also has a definite solubility in Li metal, thus allowing the surface gold to dissolve into Li to form a buffer layer for the following Li deposition. As a result, the nucleation barrier is decreased and the overpotential is significantly dropped to near 0 V on Au. Their further studies revealed the connection between Li nucleation overpotential on various metal substrates and their solubility in Li (Figure 4A), that is, zero overpotential is needed for Li nucleation on metals with high solubility in Li metal (Au, Ag, Zn, Mg), small but observable overpotential on metals having relatively small solubility in Li metal (Al, Pt), and significant nucleation overpotentials on substrates with no solubility in Li metal (Cu, Si, Sn, Ni, C). Ye and co-workers reported a uniform Al coating layer on the Cu matrix by the magnetron sputtering treatment.[62] The binary Li–Al alloy after lithiation acts as lithiophilic sites for Li nucleation, thus realizing a decreased overpotential and dendrite-free Li plating. Cui and co-workers modified planar Cu collectors with lithiophilic Ag nanoparticles through a simple substitution reaction, which serves as nucleation seeds to guide uniform lithium deposition with a cobblestone-like shape.[63] Similarly, Wang and co-workers fabricated a Sb-modified 3D Cu skeleton via a facile displacement reaction.[64] The generated lithiophilic Li–Sb interphase significantly decreased the Li nucleation barrier and promoted the Li deposition into the microchannels.

Facile fabrication of functional current collectors is highly desirable for the scaled-up application. Zhang and co-workers fabricated a lithiophilic CuZn current collector through chemical dealloying of commercial brass.[67] The Zn component in the upper surface was removed to form a porous layer, and the residual CuZn phases can induce Li nucleation in the pore to restrain the growth of Li dendrite. Recently, Suo's group explored an epitaxial induced plating current-collector (E-Cu) to prolong the lifespan of LMB.[65] An alloying reaction occurs between the liquid metal layer (Ga:In:Sn = 68.5:21.5:10) on Cu foil and Li upon lithiation, generating an epitaxial induced layer with fast Li^+ diffusivity. Therefore, Li-ions can transfer flexibly along with the alloying layer instead of plating at a fixed site with dendrites formed (Figure 4B). Besides, FSI^- in the electrolyte decomposed to form LiF in SEI, which is favorable for uniform Li plating. Benefiting from these two merits, E-Cu allowed more uniform and denser Li deposition (Figure 4C). Electrochemical tests demonstrated a high initial CE of 98.24%,

in comparison with 93.24% of the bare Cu counterpart under 0.5 mA cm^{-2} and a capacity of 5 mA h cm^{-2} (Figure 4D).

3.2.2 | Metal compounds modification

Besides alloying metal, forming an oxidation layer on the Cu surface is another facile approach to improve the lithiophilicity. Zhang and co-workers fabricated Cu_2O nanoparticles on planar Cu foil through facile air annealing, which would react with Li to produce Cu and Li_2O.[68] The overpotential of lithium nucleation on modified Cu foil was significantly decreased from 59.8 to 28.8 mV, compared with counterpart of bare Cu foil. Zhang and co-workers fabricated vertically aligned CuO nanosheets on a planar Cu foil by a simple wet chemical reaction.[69] Besides the improved lithiophilicity by CuO, the vertically aligned nanosheet structure homogenized the distribution of Li^+ flow and lowered the local current density. After that, based on the vertically aligned CuO nanosheets, Wu and co-workers further reported the use of nitrogen plasma to treat the CuO nanosheet-decorated Cu foil.[70] The plasma-induced nitrogen doping provided abundant active sites for lithium nucleation and improved the electrical conductivity simultaneously.

ZnO-based modifications have also been reported in enhancing the electrochemical performance of the Cu current collector. After the formation of elemental Zn and Li_2O, Li–Zn alloy can be produced upon further lithiation, which provides smooth Li^+ transportation channels and homogenizes the nucleation sites.[71] Zhang and co-workers developed a 30 nm-thick ZnO layer on the Cu skeleton by atomic layer deposition (ALD).[72] The as-fabricated anode showed an average CE of 98.7% over 300 cycles at 1 mA cm^{-2}. A facile air annealing method was proposed by Huang and co-workers for the in-situ growth of ZnO nanoparticles on brass.[73] Surface oxidation reactions and following replacement reaction between CuO and Zn would release the chemical energy. Due to the relatively low stacking fault energy of the brass, it would drive the surface atom diffusion. ZnO nanoparticles are thus uniformly coated on the surface of brass, which can effectively decrease the overpotential of Li nucleation.

Although metal oxides have attracted intensive research attention for current collector modification, the lithiation product, Li_2O, shows poor ionic conductivity. Li_2S, Li_3P, and Li_3N demonstrate much-improved ion conduction capability. Thus, metal sulfides, metal phosphides, and metal nitride can be promising alternatives for current collector modification. Zhai and co-workers fabricated hollow Cu_2S nanotubes on Cu foam based on the Kirkendall effect, through the

sulfurization of Cu(OH)$_2$ nanowires.[74] During the initial galvanostatic electroplating, the Li$_2$S layer was developed in situ through the replacement of Cu$^+$ in the Cu$_2$S by Li$^+$. The formed Li$_2$S layer can improve the stability of SEI and provide fast transport for Li-ions because of its high ionic conductivity. Therefore, the accumulation of Li$^+$ and the unfavorable top growth of Li are effectively avoided. Zhu and co-workers fabricated Ag$_2$S nanoparticles decorated Ni framework through a silver mirror reaction and sulfurization reaction.[75] During Li deposition, Ag$_2$S would react with Li to produce Li$_2$S and Ag. In addition to the high ionic conductivity of Li$_2$S, the produced Ag could further react with Li to form an Ag–Li alloy, which owns high bonding energy with Li. Therefore, Li nucleation sites were homogenized, and Li deposition was guided into the Ni framework. Compared with CuO and Cu$_2$S, Cu$_3$P has better electrical conductivity and lithiophilicity derived from its stronger interaction with Li. Moreover, the Li$_3$P formed by the initial reaction of Li$^+$ and Cu$_3$P has a high ionic conductivity of 10^{-4} S cm^{-1}, which is crucial for the fast Li-ion transport at the electrode surface. Through the reaction of Cu nanowire with phosphine vapor, Zhang and co-workers fabricated a 3D current collector with phosphide gradient along the cross-section of the current collector.[66] The phosphide gradient was formed because of the decreased concentration of phosphine gas in nanowires from the top to bottom (Figure 4E). It helps achieve well-balanced conductivity and lithiophilicity. Consequently, uniform Li nucleation sites and dense Li deposition were realized within the skeleton. An oriented texture of deposited Li on the surface is therefore formed within the spatial confinement from the adjoining Li crystals (Figure 4F). Similarly, Lei and co-workers fabricated a lithiophilic Co$_3$N nanobrush on a Ni foam, also enabling dendrite-free Li deposition.[76]

In recent years, the merits of LiF-enriched SEI have been widely reported, in terms of the rapid transport of Li$^+$ ions, inhibition of Li dendrite growth, and improved electrochemical performance in lithium batteries.[77] Metal fluoride-based modification is an effective method to form LiF-rich SEI. Zhang and co-workers fabricated a LiF-protected planar Cu foil to realize columnar and uniform Li deposition.[28] The amorphous LiF-rich surface was formed on Cu foil by in-situ hydrolysis of lithium hexafluorophosphate. Because of the low diffusion energy barrier of the LiF layer, Li ions can transfer quickly along the surface and be reduced by electrons to form dense nucleation sites. The aligned columnar structure was achieved by the initial horizontal growth near the nucleation sites and following vertical growth because of the spatial confinement (Figure 4G). When used as an anode current collector, the LiF-modified Cu foil shows a high average CE of 98.7% over 120 cycles. Similarly, Huang and co-workers prepared an interconnected NiF$_x$ nanosheet decorated Ni foam through a one-step fluorination method.[78] Because of the superior lithiophilicity of the NiF$_x$ and in-situ formed LiF-enriched SEI layer, the nucleation barrier is greatly decreased from 75 mV to 32 mV, compared with bare Ni foam.

3.3 | Carbon-based modification

Carbonaceous materials are promising alternatives for modifying metal current collectors because of their (electro)chemical stability, great variety of structures, and diversified synthesis strategies. Many carbonaceous modification materials have been reported so far, including zero-dimensional nanodiamonds,[79] one-dimensional nanofibers,[80] two-dimensional graphenes,[81–87] and three-dimensional carbon architectures.[30,88–91]

3.3.1 | 0D and 1D carbon-based modification

Liu and co-workers fabricated a double-layer nanodiamond film-modified Cu substrate through the microwave-plasma chemical vapor deposition method (Figure 5A).[79] Because of the unique properties of the as-prepared nanodiamond film, including the nanoporous structure, weak adhesion with the Cu substrate, electrical insulation nature, and high electrochemical stability, Li uniformly deposits below the interface layer. The underneath deposition mode effectively avoids the side reactions between the electrolyte and Li metal. The high elastic modulus of the film (over 200 GPa) suppresses the dendrite growth during the Li plating process. Moreover, the COMSOL simulation demonstrated that the localized high concentration Li$^+$ caused by defects in one layer can be shielded by the other (Figure 5B). Therefore, the double-layer design can effectively improve the uniformity of Li-ion flux and avoid the growth of Li dendrite near defect sites. A 3D carbon nanofiber (CNF) network-modified Cu foil was proposed by Zhang and co-workers through a facile vacuum filtration strategy.[80] The large surface area of CNF decreases the local current density and the good flexibility of CNF can accommodate the volumetric change of LMA during Li plating/stripping cycles. Besides, the graphitic structure of CNF provides many active sites for reversible Li-ion insertion upon initial lithiation, which promotes the subsequent uniform Li deposition.

3.3.2 | 2D graphene-based modification

Graphene owns large surface area, high flexibility and mechanical strength, as well as abundant defects and interlayer voids as Li$^+$ diffusion channels. Yang
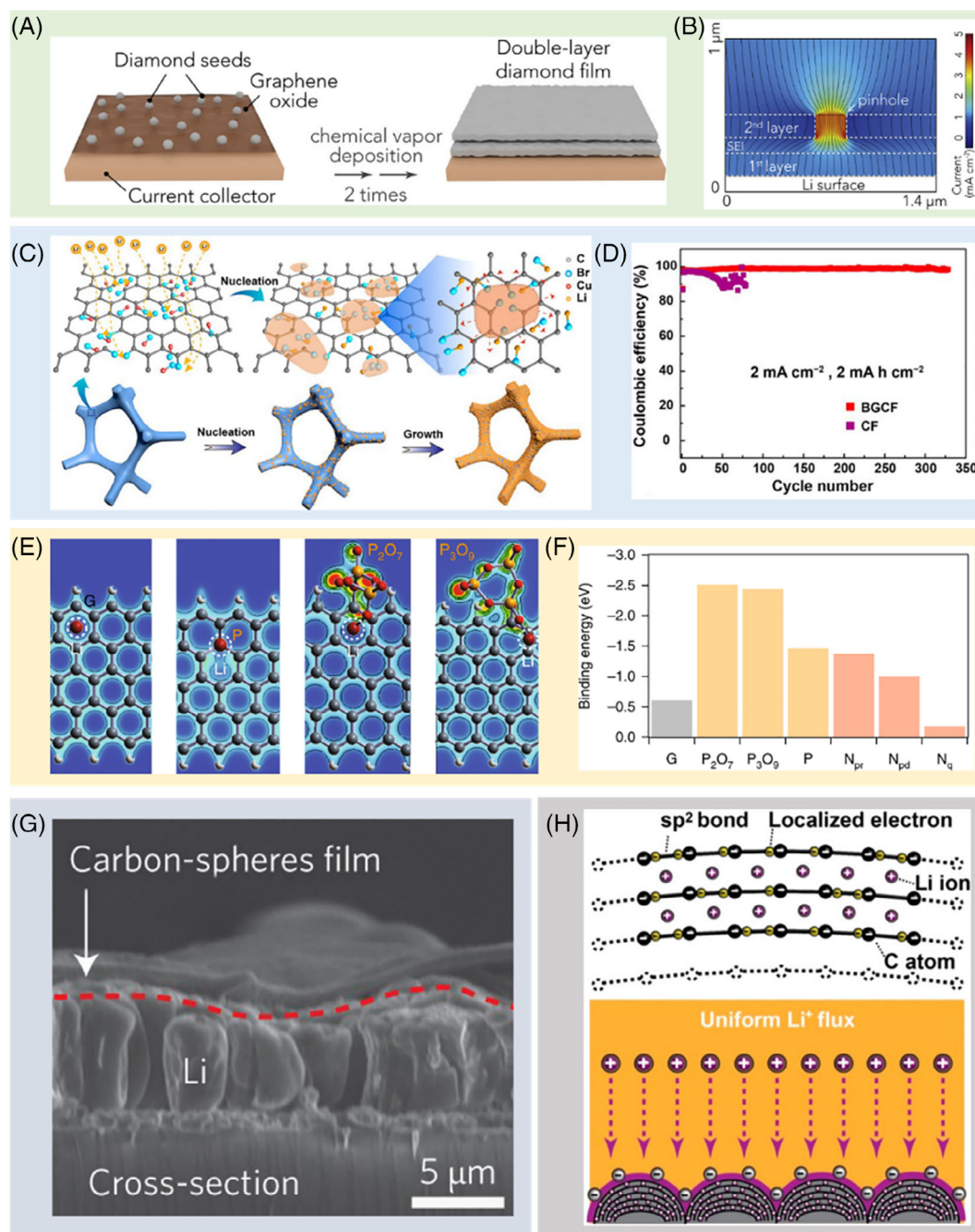
FIGURE 5 (A) Schematic diagrams of fabrication of a double-layer nanodiamond film-modified Cu substrate. (B) Simulations of the Li-ion flux across double-layer nanodiamond film. Reproduced with permission: Copyright 2018, Elsevier.[79] (C) Schematics of Li metal deposition on Br-doped and CuBr-decorated graphene-modified Cu foam. (D) Comparison in Coulombic efficiency of Cu foam and Br-doped and CuBr-decorated graphene-modified Cu foam. Reproduced with permission: Copyright 2018, American Chemical Society.[81] (E) Two-dimensional local charge density profiles along with a projection of charge densities for Li atom adsorption on graphene, phosphate-functionalized reduced graphene oxide, P_2O_7-modified graphene, and P_3O_9-modified graphene. (F) Binding energies between the Li atom and graphene (G), P_2O_7, P_3O_9, bulk phosphorus (P), pyrrolic (Npr), pyridinic (Npd), and quaternary (Nq) species. Reproduced with permission: Copyright 2018, Springer Nature.[82] (g) Cross-sectional view SEM image of deposited Li under the hollow carbon nanosphere thin film. Reproduced with permission: Copyright 2014, Springer Nature.[30] (H) Schematic illustration of Li^+ flux distribution on onion-like, graphitized spherical carbon granules. Reproduced with permission: Copyright 2017, American Chemical Society[90]

and co-workers developed a graphene coating layer on a Cu foam through a facile drying process followed by thermal annealing.[85] The as-constructed skeleton not only shows a moderate surface area to effectively decrease the local current density but also presents an improved lithiophilicity. Therefore, it enables a much lower polarization

and nucleation overpotential than bare Cu. Hence, a conformal and smooth Li deposition was obtained. Similarly, a pie-like skeleton constructed by graphene warped Cu nanowires was reported by Yan and co-workers.[84] The outside graphene layer not only suppressed the Li dendrite due to its excellent mechanical strength but also reduced the interfacial resistance because of its high electrical conductivity. Moreover, the abundant defects produced in graphene nanosheets during hydrogen reduction allow smooth Li-ion diffusion through the graphene shell.

Li dendrite growth is mainly caused by the heterogeneous distribution of electrons and Li^+ flux. Hetero-element-doped graphene could enable a stronger interaction with Li^+ in the electrolyte. Zhang and co-workers reported nitrogen-doped graphene in the modification of porous Cu current collector, which can effectively regulate the initial Li nucleation process.[86] The abundant nitrogen functional groups offer high binding energies with Li atom, resulting in a uniform Li^+ flux. Wan's group modified Cu foam by Br-doped and CuBr-decorated graphene through the surface-assisted Ullmann reaction of hexabromobenzene.[81] Because of the high binding energy between the Li atoms and the Br-doping sites, the electrode surface shows an excellent lithiophilicity, which can homogenize the Li^+ flux and decrease the Li nucleation overpotential under high current densities, and further prompt homogeneous Li nucleation (Figure 5C). Moreover, LiBr was generated upon lithiation of CuBr. It provided a fast Li diffusion pathway to adjust pancake-like Li nucleation seeds, which greatly suppresses the side reactions between the electrolyte and Li metal. As a result, the modified skeleton shows an average CE of 98.8% over 300 cycles at a current density of 2 mA cm^{-2} and an areal capacity of 2 mAh cm^{-2} (Figure 5D). A phosphate-functionalized reduced graphene oxide (PrGO)-modified Cu foil was created by Kim and co-workers.[82] As shown in Figure 5E,F, P_2O_7 and P_3O_9 functionalized graphene have higher binding energies with the Li atoms than graphene, N-doped graphene, and P-doped graphene. Projected charge densities after Li atom adsorption on those different structures are also different. In terms of graphene, the Li atom would be adsorbed at the center of the honeycomb. For P-doping graphene, because of the extra electron of P and a relatively bigger atomic radius of P than C, the Li atom tends to be adsorbed by P. While in the case of phosphate-functionalized graphene, P_2O_7 and P_3O_9 act as lithiophilic sites because of the presence of a free electron pair. It forms a localized and uniform charge cloud, which can strongly attract Li^+ from the electrolyte. Thanks to these features of PrGO, uniform Li^+ flux and dendrite-free Li deposition were achieved.

3.3.3 | 3D carbon architectures-based modification

Because of the electronically conductive nature of graphene, Li deposits on its surface. Such a "surface growth" mode could exacerbate the consumption of electrolytes and the generation of lithium dendrites. To realize a more favorable "bulk growth" mode, Zheng and co-workers developed a monolayer of interconnected amorphous hollow carbon nanospheres on the Cu substrate by using vertically deposited polystyrene nanoparticles as a template.[30] The as-formed amorphous carbon film is chemically stable with Li metal and it has an Young's modulus of ~200 GPa, which is high enough to inhibit the growth of dendrite. Besides, the loose attachment with the Cu foil allowed the hollow film to be easily lifted and Li would deposit underneath the amorphous carbon film because of its low electronic conductivity. Owing to these merits, the deposited Li metal shows a column-like morphology without long filaments or dendrites (Figure 5G). The electrochemical tests showed an average CE of 99% over 150 cycles at 1 mA cm^{-2} for the as-fabricated anode. Xu and co-workers synthesized N, O-codoped vertically aligned carbon sheet arrays on Cu foil, which effectively homogenize the Li^+ flux and the electrical field.[91] The lithiophilic nitrogen/oxygen dopants of the carbon sheet enable the uniform Li nucleation inside the vertical channels. As a result, a long-life Li plating/stripping over 1300 h was achieved, with an average CE above 98% at 0.5 mA cm^{-2} and 1.0 mAh cm^{-2}.

Ye and co-workers fabricated some onion-like, graphitized spherical carbon granules on Ni foam by CVD method, with nanogap formed between the graphitized carbon layers (Figure 5H).[90] During the Li deposition, Li ions are firstly intercalated in the graphite layers and then deposited into the nanogaps. Because of the curved surface, the delocalized π electrons of C atoms become partially localized, resulting in enhanced negativity. Moreover, the formed Li/C compounds could further increase the negativity of the carbon surface. It ensures a stronger binding between the carbon surface and Li ions in the electrolyte, which is beneficial for the homogenization of the Li^+ flux. Besides, the Li/C compounds can provide some excessive Li during redox cycling. When the graphitic carbon-modified Ni foam electrode is coupled with a lithium iron phosphate (LiFePO$_4$) cathode, the full cell shows an ultralong lifespan of 1000 cycles at a Li surplus of merely 5%.

3.4 | Organic-based modification

Materials containing organic functional groups have been widely employed to modify current collectors of LMBs. Their (electro)chemical inertness, good mechanical

properties, and generally lithiophilic features enable effective inhibition of Li dendrite growth and the homogenous Li deposition.[92,93]

3.4.1 | Polymer materials-based modification

A polyethylene oxide (PEO) thin film was fabricated by Assegie and co-workers to modify the Cu current collector, which shields the deposited Li from contact with the extraneous electrolyte and promotes the formation of a thin and robust SEI layer.[94] It also enables the homogenous Li-ions flux due to the impressive interaction between Li ions in the electrolyte and the polar oxygen atoms at the surface of the PEO film. Likewise, Luo and co-workers proposed a thin β-PVDF film coating, whose abundant functional groups offer a strong affinity to Li^+ enabling an even Li^+ flux.[95] The alignment of F atoms in β-PVDF also enhances the interaction between the electronegative C-F functional groups and Li atoms at the interface, favoring the layer-by-layer Li deposition. Liu and co-workers synthesized a polyimide (PI) skeleton with vertical channels to modify the stainless steel current collector.[96] The vertical-aligned nanochannels with a high aspect ratio divide the space into many small confinements. The Li^+ flux was confined in the nanochannels and isolated from each other, so the uncontrollable growth of Li dendrite in one site was avoided with homogeneous Li nuclei distribution and growth achieved. (Figure 6A). At the initial stage of Li plating, Li metal could deposit into the vertical-aligned nanochannels first. After the nanochannels were fully occupied, further Li deposition occurred on the top surface with a columnar, smooth, round morphology generated, as shown in Figure 6B.

Apart from the ordinary rigid polymer films, functional coating layers with viscoelastic behaviors have also attracted much attention because of their adaptability to the large volume change during Li plating/stripping. Liu and co-workers synthesized a silly putty (SP) film through dynamic crosslinking of polydimethylsiloxane (PDMS) chains by the boron-mediated cross-links.[100] Because of the deformation and reconnection of the cross-links, as-fabricated SP film shows a "solid–liquid" hybrid behavior, and it can reversibly switch between its "liquid" and "solid" states based on the rate of lithium growth. Therefore, it can act as a smart dynamic protection layer toward uniform Li deposition. Similarly, the same group fabricated a highly viscoelastic polymer film containing abundant hydrogen bonding groups.[101] This functional coating layer effectively prevented the formation of cracks or pinholes in the SEI layer, avoiding the creation of "hot spots". Yu and co-workers fabricated a

dynamic single-ion-conductive network (DSN) through the Al-OR (R = soft fluorinated linker) bonding to modify the Cu foil.[97] The tetrahedral Al $(OR)_4^-$ crosslinking centers in the DSN layer act as dynamic bonding motifs and counter anions for Li^+, resulting in the high Li^+ conductivity of the as-fabricated film (Figure 6C). Therefore, the DSN layer not only decreased the electrolyte penetration and avoided the parasitic reactions between metal Li and electrolyte but also ensured a low interfacial impedance and overpotential during Li plating/stripping. Besides, the low coordination bonding energy of the Al-O bond endows the viscoelasticity and dynamic properties of the DSN coating, which allows the formation of a conformal protection layer on the deposited Li. Consequently, the DNS-modified electrode showed an average CE of 97.3% over 400 cycles at 0.25 mA cm^{-2} with an areal capacity of 0.5 mAh cm^{-2}.

Inducing lateral lithium deposition is another effective approach to achieve safe lithium metal batteries.[98,102] Zou and co-workers fabricated a PI-clad copper grid current collector through hot lamination, laser ablation, and subsequent alkaline etching treatments.[98] The pinholes in the upper PI layer ensure smooth diffusion of electrolyte and distortion of the electric field distribution. It resulted in a unique lateral pattern, where the electric field propagates from the counter Li electrode, through the pinholes of the PI layer, and extends laterally to the inner surface of the Cu scaffold, as suggested by the simulation using an electrical conduction model (Figure 6D). Therefore, Li dendrites would grow along the direction parallel to the separator. The PI layer also worked as a physical barrier to confine the growth of Li dendrites inside the hollow compartments. Thus, the cells could safely operate in a limited cycling capacity even with dendrites grown. As a result, the prepared electrode showed an average CE of ~99% over 150 cycles at 0.5 mA cm^{-2} with a cycling capacity of 0.5 mAh cm^{-2}.

3.4.2 | MOFs and COFs-based modification

Metal–organic frameworks (MOFs)[103−106] and covalent organic frameworks (COFs)[99,107] have gained increasing attention for functional modification of current collectors, because of their unique tunable functionality and designable structure.[93,108,109] Qian and co-workers synthesized Nano-MOF-199 to act as a robust shield to suppress the growth of lithium dendrite on Cu foil.[106] Besides, the high-polarity structure of Nano-MOF-199 layer can effectively homogenize the Li^+ flux toward uniform lithium deposition. Recently, the electrically conductive Ni_3(2,3,6,7,10,11-hexaiminotriphenylene)$_2$ ($Ni_3[HITP]_2$) was fabricated to modify Cu foil current
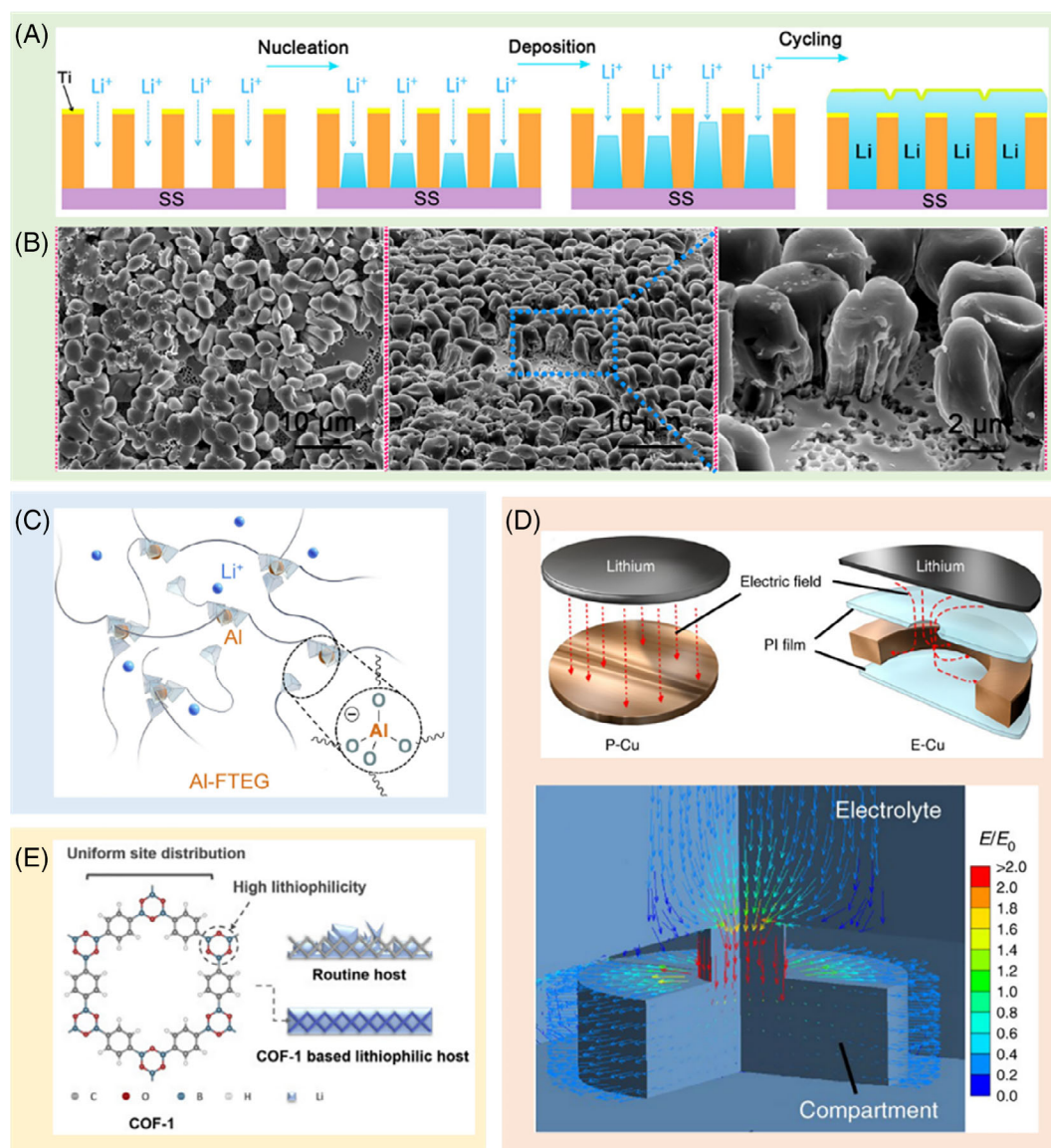
FIGURE 6 (A) Schematic diagrams of Li deposition on polyimide skeleton with vertical channels modified stainless steel current collector. (B) SEM images of lithium deposited on polyimide skeleton with vertical channels modified stainless steel current collector. Reproduced with permission: Copyright 2016, American Chemical Society.[96] (C) Conceptual sketch of a dynamic single-ion-conductive network. Reproduced with permission: Copyright 2019, Elsevier.[97] (D) Schematic illustration and the simulated result of the electric field distribution in PI-clad copper grid (E-Cu). Reproduced with permission: Copyright 2018, Springer Nature.[98] (E) Schematic illustration of COF-1 and deposition on COF-1. Reproduced with permission: Copyright 2020, Elsevier[99]

collectors by Zhao and co-workers.[105] The $Ni_3(HITP)_2$ film has a "honeycomb"-like architecture, which provides a large specific surface area to decrease the local current density. In addition, the nitrogen-containing functional groups exhibit an excellent lithium affinity, promoting homogenous Li deposition.

COFs exhibit much higher chemical stability compared with MOFs because the small molecular units in COFs are bound by strong covalent bonds.[110] Xu and co-workers fabricated COF-LZU1, in which the aldehyde function groups interact with the bis(trifluoromethanesulonyl)imide to

immobilize anions, alleviating the space charge effect.[107] Besides, the imine bonds on COF-LZU1 can improve the lithiophilicity to homogenize the Li-ions flux. Song and co-workers synthesized a boroxine COF-1 through a solvothermal method.[99] The boroxine rings in COF-1 have ideal lithiophilicity because of the strong ion-dipole interactions with Li atoms, which greatly decreases the nucleation over-potential. Besides, the homogenous atomic-scale distribution of well-defined boroxine rings is beneficial for guiding quite uniform Li deposition (Figure. 6E). Consequently, a composite was fabricated with COF-1 and graphene as an

anode. It showed low nucleation overpotentials of 8.7, 19.8, and 38.8 mV at 0.5, 1.0, and 3.0 mA cm^{-2}, respectively. This anode also displayed a high average CE of 98% over 240 cycles at 1.0 mA cm^{-2} with an areal capacity of 1.0 mAh cm^{-2}.

3.5 | Other modifications

In addition to the above-mentioned metal-, carbon-, and organic-based decorations, the development of novel modification materials, for example, graphitic carbon nitride (g-C$_3$N$_4$),[111,112] hexagonal boron nitride (h-BN),[113,114] and garnet-type materials,[115] have also drawn increasing attention to afford the current collectors with attractive functionalities. A 2D g-C$_3$N$_4$ nanosheets coated Ni foam was prepared by Lu and co-workers through thermal polymerization.[112] The tri-s-triazine units of g-C$_3$N$_4$ afford abundant Li nucleation sites that can naturally form a ring-shaped micro-electric field, as suggested by the DFT calculation (Figure 7A). The as-generated micro-electric field effectively improves the Li affinity of the modified Ni foam, resulting in a decreased Li nucleation overpotential (Figure 7B). Similarly, a single-crystalline α-Si$_3$N$_4$ submicron-wire membrane, reported by Li and co-workers, also affords abundant polar covalent bonds at the surface, serving as efficient anchoring points to attract Li$^+$ from the electrolyte.[116] Zhai and co-workers further constructed a 3D current collector consisting of g-C$_3$N$_4$/graphene/g-C$_3$N$_4$ sandwiched nanosheets.[111] The insulating g-C$_3$N$_4$ can inhibit Li deposition on the surface, inducing Li plating in the van der Waals gap between graphene and g-C$_3$N$_4$. Moreover, the uniform lithiophilic sites of g-C$_3$N$_4$ can further homogenize the Li-ions flux.

h-BN is chemically inert and has a high theoretical in-plane Young's modulus. Each hexagonal ring in h-BN owns a pore size of only ~1.2 Å, smaller than the diameter of Li$^+$ ions (~1.8 Å) and Li atoms (~2.7 Å). Hence, Li$^+$ ions cannot diffuse through the ring pore. The deposited Li metal cannot move through the layer. Xie and co-workers synthesized a 2D h-BN layer via CVD to protect Cu current collector.[114] The point and line defects of 2D h-BN allow Li$^+$ ions to penetrate through the layer and then deposit on Cu foil as the physical interaction between h-BN and Cu is weak. However, the fabricated 2D h-BN layer was polycrystalline, leading to holes generated at the grain boundaries after Li plating. To address this issue, they further proposed a selective ALD of LiF on CVD-grown h-BN.[113] The LiF deposited preferentially on the defect sites and void space, generating seams to fasten firmly the h-BN crystallites. Consequently, the LiF linkers enhanced the mechanical strength of the hybrid LiF/h-BN film, which can effectively inhibit the growth

of Li dendrites to achieve a smooth and uniform morphology of plated Li (Figure 7C).

The garnet-type Li$_{6.4}$La$_3$Zr$_{1.4}$Ta$_{0.6}$O$_{12}$ (LLZTO) has a high Li-ion conductivity and good (electro)chemical stability. Li and co-workers fabricated a 3D Cu/LLZTO interface with LLZTO strongly anchored on the Cu foam surface to serve as an artificial SEI.[115] The unmovable SEI layer can effectively accommodate the volume change during Li plating/stripping, achieving impressive electrochemical performance for Li anode. In another work, through infrared laser treatment, the silicone-based adhesive of a Kapton polyimide tape was converted into a homogeneous porous SiO$_x$ layer on Cu.[117] The coated SiO$_x$ layer has a lithiophilic surface, a high modulus, and a large surface area. All the properties help to inhibit the growth of Li dendrites and suppress the formation of inactive Li particles.

Recently, different crystal lattices on the Cu surface were found to result in distinct priorities for Li deposition. The commercial Cu current collectors have multiple grains with different surface facets on a submicron scale. The Cu (111) surface is dominant among the three major facets of (100), (110), and (111), because of its lowest surface energy. Kim and co-workers demonstrated that the Cu (100) plane was the most favorable one for Li nucleation among the three major facets because of the lowest Li nucleation potential barrier.[118] Compared with a conventional Cu foil with randomly oriented surface facets, the fabricated (100) plane-majored Cu current collector showed a higher Li nuclei density, consequently resulting in a twofold increase in the Li plating/striping cycling stability. Gu and co-workers also reported that the fcc Cu (100) faces have good surface lattice matching with bcc Li (110) faces, which can further guide Li bulk deposition along the most stable <110 > direction.[119] Later on, Fu and co-workers treated Cu nanowires with a sodium formate solution to reconstruct the dominated surface of Cu from Cu (111) into Cu (110).[120] A passivation layer composed of [Cu$_2$(HCOO)$_2$(OH)$_4$] dimers and OH$^-$ groups was formed on the surface of the Cu (110) plane, which increases the lithiophilicity and oxidation resistibility of Cu current collectors.

To summarize, 3D current collectors could serve as high-surface-area alkali metal hosts to accommodate the volume fluctuation, reduce the local current density and facilitate the even distribution of Li$^+$ flux. The mechanical strength of 3D metallic current collectors still needs to be enhanced, and their large-scale fabrication costed still need to be reduced. Modification on the current collector surface by functional materials could effectively drop the Li nucleation barrier and facilitate homogeneous nucleation. But such merits would gradually be weakened under practical testing conditions (high
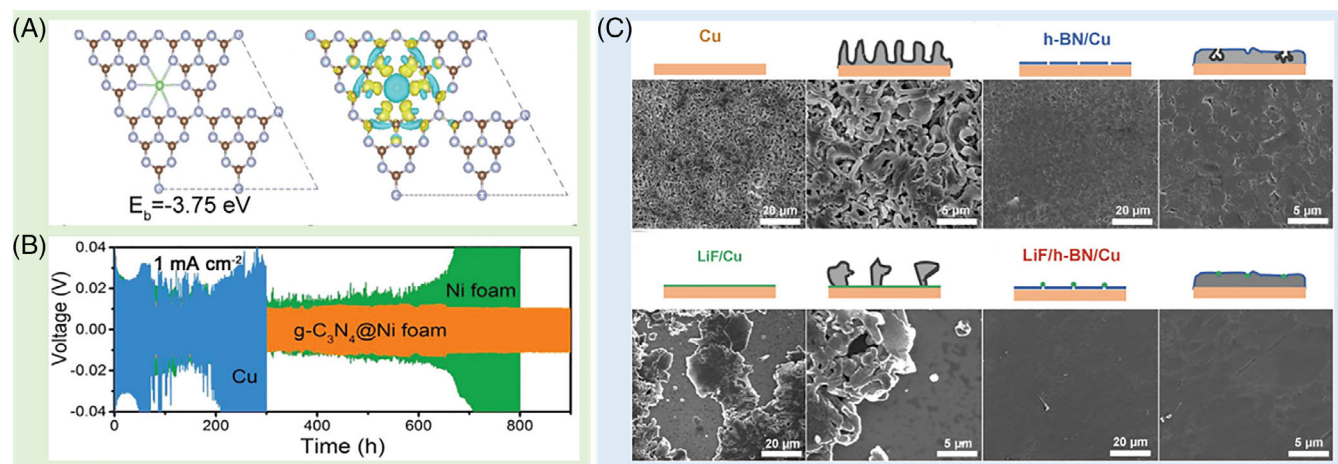
FIGURE 7   (A) Crystal models of a Li$^+$ adsorbed on g-C$_3$N$_4$ and the corresponding charge density difference. (B) Voltage–time profiles of Li plating/stripping on g-C$_3$N$_4$@Ni foam, Ni foam, and Cu electrodes at 1.0 mA cm^{-2} with 1.0 mAh cm^{-2} in a symmetrical cell. Reproduced with permission: Copyright 2019, John Wiley & Sons, Inc.[112] (C) Schematics and SEM characterization of Li plating on Cu, h-BN/Cu, LiF/Cu, and LiF/h-BN/Cu current collectors. Reproduced with permission: Copyright 2017, the American Association for the Advancement of Science[113]

current rate and high areal capacity) because of the rapid accumulation of dead Li, which blocks the Li$^+$ diffusion channels to lithiophilic sites.

4 | ADVANCED CARBONACEOUS CURRENT COLLECTORS FOR LMAS

Carbon materials have been widely used as current collectors in LMBs because of their high electrical conductivity, superior (electro)chemical stability, and light-weight.[121] Pure carbon materials, like carbon fiber and carbon nanotubes, were used to construct 3D architecture with various heteroatoms employed to improve the lithiophilicity of carbon materials. Some metals and metal compounds were also used to increase the affinity of lithium ions and current collectors.

4.1 | Pure carbon and heteroatom-doped carbon current collectors

Liu and co-workers fabricated a 3D hollow carbon fiber (3D-HCF) current collector with a high electrochemically active surface area.[27] With the increase of areal capacity during Li deposition, the wall thickness of the tubular fibers gradually increased. It indicates that part of the Li metal deposited inside the tubular fibers, and thus dendrite growth was well inhibited (Figure 8A). The as-fabricated 3D-HCFs-based anode exhibited high and stable Coulombic efficiencies (~99.5% over 350 cycles), large areal capacity, and long-running lifespan (>1200 hrs).

Similarly, a carbon nanotube (CNT) sponge was adopted as a 3D current collector by Yang and co-workers.[122] Lithiation at potential above 0 V versus Li$^+$/Li enhances the lithiophilicity of the CNT sponge, which significantly decreases the Li nucleation overpotential and leads to a homogeneous Li deposition.

Introducing heteroatom dopants into carbonaceous materials is an effective approach to improve their Li affinity. Zhang and co-workers fabricated nitrogen-doped graphene (NG) matrix by annealing graphene in an ammonia atmosphere.[32] The lithiophilic N-containing functional groups, including pyridine nitrogen, pyrrolic nitrogen, and quaternary nitrogen, guide the uniform Li nucleation. Therefore, the NG-based electrode exhibited a dendrite-free Li deposition morphology after prolonged cycling. Similarly, a 3D nitrogen-doped graphitic carbon foam was synthesized by Liu and co-workers. They achieved a low overpotential of 62 mV even when the deposition of Li was at a high current density of 10 mA cm^{-2}.[125] Through first-principles simulations, Wang and co-workers find that sulfur atom doping could effectively enhance the Li adsorption ability of graphene.[123] In sulfur-doped graphene (SG), the doped S atom sacrifices the adsorption ability in a single atomic site, but uniformly improves the adsorption energies in a larger surrounding area. Therefore, SG owns a much-improved lithiophilicity than pristine graphene. Electrochemical tests demonstrated that the SG-based electrode shows a high average CE of 99% over 180 cycles at 0.5 mA cm^{-2} and an ultralow overpotential of 5.5 mV (Figure 8C). To realize long-life and high-rate LMBs, a single-atom Ni-supported nitrogen-doped graphene
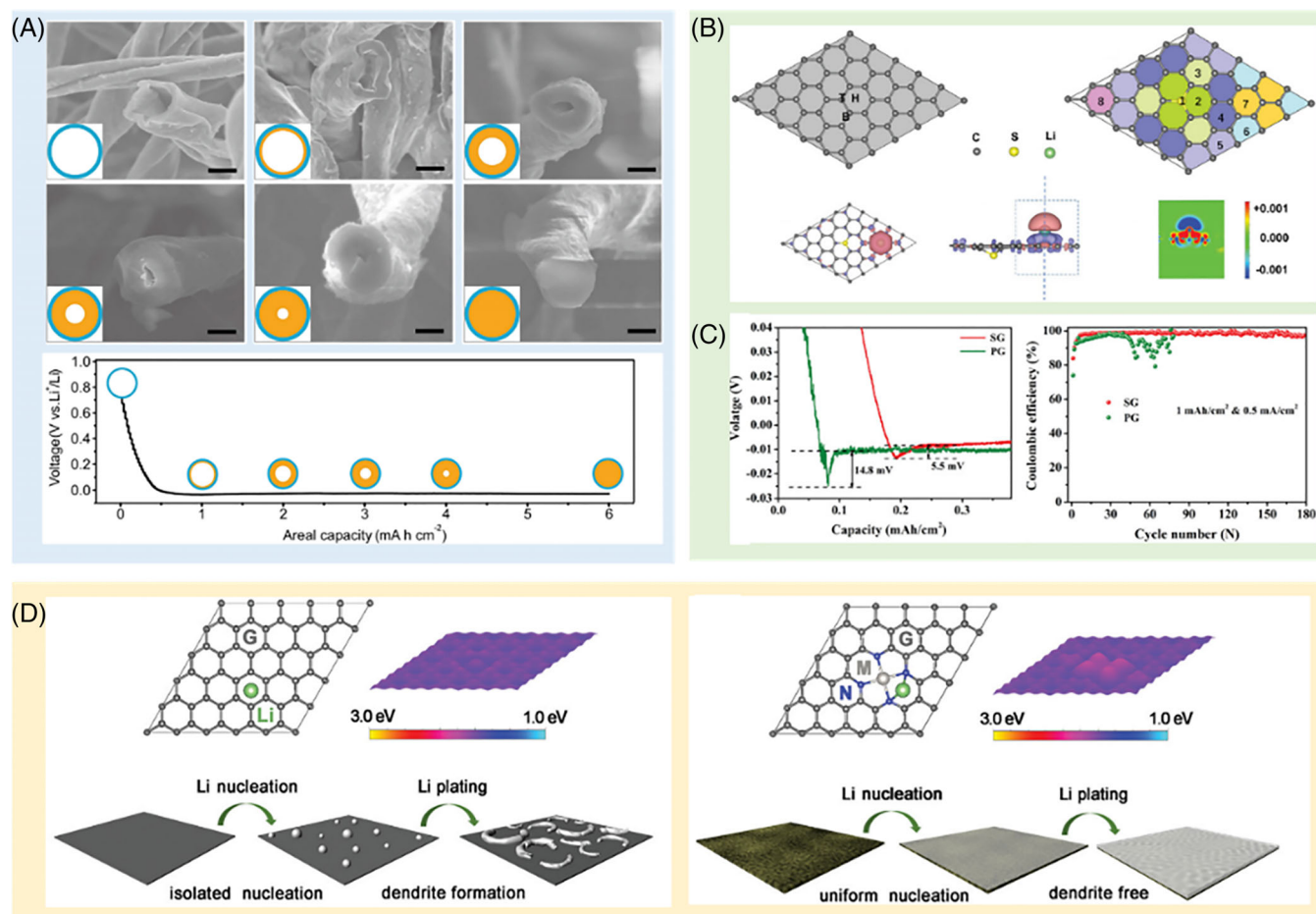
FIGURE 8 (A) Cross-sectional view SEM images of 3D-HCFs with different lithium deposition areal capacities. Reproduced with permission: Copyright 2017, Elsevier.[27] (B) The charge density distribution of SG with one Li atom adsorbed. (C) The voltage–capacity curves during Li nucleation and the CEs of cycling for PG and SG electrode. Reproduced with permission: Copyright 2019, John Wiley & Sons, Inc.[123] (D) Li adsorption energy distribution and schematic illustration of Li deposition process on the pristine graphene and a single-atom Ni-supported nitrogen-doped graphene electrode. Reproduced with permission: Copyright 2019, John Wiley & Sons, Inc.[124]

matrix was fabricated by Zhai and co-workers through two-step pyrolysis in an argon atmosphere.[124] The isolated metal atoms are coordinated with nitrogen atoms, and the Li adsorption energy in the localized area around metal atomic sites is increased with a moderate adsorption energy gradient because the formation of M-N$_x$-C sites (M, N, and C denoted as metal, nitrogen, and carbon atoms, respectively) increases the atomic structural stability (Figure 8D). Therefore, the fabricated electrode can achieve uniform nucleation and dendrite-free deposition morphology.

4.2 | Metal modification

Metal elements such as Ag and Au own zero or low Li nucleation energy barrier. Therefore they can be employed as suitable seeding sites to exclusively improve the Li affinity of carbonaceous substrates.[29,126–131] For

instance, Yang and co-workers fabricated ultrafine Ag nanoparticles (AgNPs) to modify CNFs through a rapid Joule heating method (Figure 9A).[29] The ultrahigh temperature during this method ensures the strong binding between AgNPs and CNFs, which is favorable for the structural stability during long-term charge–discharge cycles. Because of the appreciable solubility of Ag in Li, the homogeneously dispersed ultrafine AgNPs can significantly decrease the Li nucleation overpotential. It can also serve as nucleation nanoseeds to guide the uniform Li deposition on CNFs (Figure 9B). In another work, an Ag nanoparticle–embedded nitrogen-doped carbon macroporous fibers hybrid host was synthesized by Fang and co-workers.[130] With the reversible solid solution–based alloying reaction between Ag and Li, the Li nucleation overpotential was greatly dropped. To realize the growth of Li deposition on the current collector, the method of modifying with Au nanoparticles (AuNPs) on the backside of carbon nanofibers (CFs) was proposed by
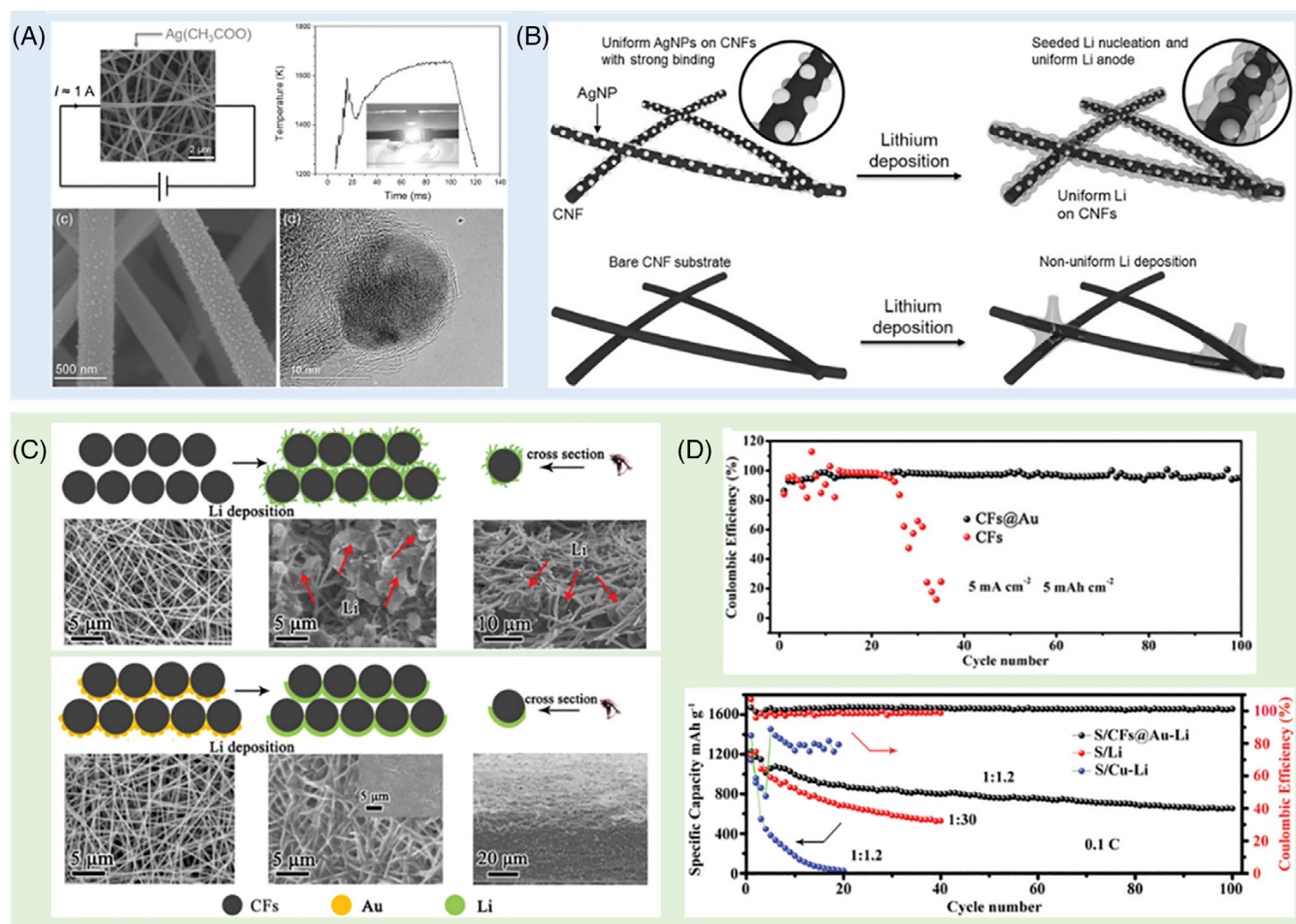
FIGURE 9 (A) Schematic illustration of the Joule heating method and SEM, and high-resolution TEM images of AgNPs dispersed on CNFs. (B) Schematic illustration of the Li deposition behavior on AgNPs-modified CNFs electrode and bare CNF electrode. Reproduced with permission: Copyright 2017, John Wiley & Sons, Inc.[29] (C) Schematic illustration and surface SEM images of CFs and CFs@Au. (D) Coulombic efficiency of CFs@Au and CFs electrodes and cycle performances of Li–S full cells with the different anodes. Reproduced with permission: Copyright 2018, Elsevier[126]

Xiang and co-workers.[126] Similar to Ag, Au can also form a buffer layer of solid solution with Li, resulting in a much lower nucleation barrier than the pure carbon substrate. Besides, because of the Li affinity of AuNPs, Li would selectively deposit on the side away from the separator (Figure 9C). Therefore, even the Li dendrite growth occurs during long-term redox cycling, the short circuit can be effectively avoided. Furthermore, the in situ formed Au-containing SEI is strong enough to prevent the side reaction and accommodate the volume change during redox cycles. As a result, a high average CE of 98.0% over 100 cycles was achieved at a high current density of $5 \, mA \, cm^{-2}$ and deposition capacity of $5 \, mA \, h \, cm^{-2}$. When paired with S, polyacrylonitrile-sulfur cathode, the Li–S full cell with CFs@Au–Li anode also exhibited good cycle performance with limited Li amount (Figure 9D).

4.3 | Metal compound modification

Diverse lithiophilic metal oxides, like ZnO and Al_2O_3, have also been proposed to modify carbonaceous current collectors.[132–134] ZnO nanoparticles confined in 3D porous carbon composite microspheres were fabricated by Tang and co-workers through a facile and scalable in-situ synthesis strategy.[134] The confinement within ultrathin carbon walls can effectively prevent ZnO nanoparticles from agglomerating and detaching from the current collectors during redox cycling. Thus, the uniform distribution and structural stability of ZnO could be maintained for continuously guiding the homogenous lithium deposition along the wall surface. In another work, Zhang and co-workers deposited a thin layer of Al_2O_3 on the CNTs surface via an ALD method.[132] The conformal Al_2O_3 deposition layer acts as an artificial SEI

to provide a stable electrode/electrolyte interface and block the growth of Li dendrites.

Because of their intrinsically low electrical conductivities, metal oxides-based modification on carbonaceous current collectors cannot realize a uniform Li distribution at a high current density.[135] Metal nitrides such as Mo_2N, CoN_x, TiN, and AlN could be more favorable.[132–138] A 3D framework configured with Mo_2N-modified CNF architecture was fabricated by Luo and co-workers via an in situ reduction nitridation method.[137] During the initial stage of Li deposition, metallic Mo and Li_3N were formed from the reduction of Mo_2N and the formed Mo phase could serve as the preferred Li nucleation sites. Therefore, Mo_2N-modified CNF could significantly decrease the Li nucleation overpotential and guide a homogeneous Li nucleation. Similarly, a CNF mat decorated with ultrafine titanium nitride (TiN) nanoparticles was synthesized by Lin and co-workers.[135] In addition to the lithiophilic properties of TiN sheath, the pseudocapacitive behavior of TiN promotes the ultrafast Li^+ storage and the charge transfer process at a high plating/stripping rate. The CNF-TiN anode so made exhibited an excellent cycling stability with CE being 98.6% after 200 cycles at a current density of 3 mA cm^{-2}. A large specific capacity of 6 mAh cm^{-2} was obtained after 100 cycles.

4.4 | Other modifications

Nafion film owns high thermal/chemical stability, good mechanical strength (Young's modulus of 0.18 GPa), and large Li-ion conductivity. Thus, it is a promising candidate of artificial SEI in LMAs. A lithiated Nafion (LNafion) layer was used to modify the inner and outer surface of lotus-root-like carbon nanofiber (LCNF) by Xiang and co-workers through a Nafion coating and subsequent lithiation process.[139] By designing a proper interior to exterior radius ratio in the hollow CNF, Li ions can selectively deposit on the inner surface of the channels because of the drifting effect from the structural stresses. The Nafion layer sticks tightly on the inner surface and the outer surface of the LCNF, as shown in images of EDX element distribution (Figure 10A). With the modification of LNafion, the side reactions between Li metal and electrolyte were effectively suppressed with an average CE of 98% achieved even at high current densities of 5 and 8 mA cm^{-2}. In another work, Xu and co-workers fabricated a $g-C_3N_4$ layer evenly coated commercial carbon cloth (CC) through a simple thermal condensation reaction.[33] The lithiophilic $g-C_3N_4$ layer served as the artificial interphase, which can guide uniform Li^+ distribution and eliminate the "hot spots" where the dendrites would be produced. Besides, the insulative nature of the $g-C_3N_4$ layer promotes interlayered Li deposition between the $g-C_3N_4$ and CC (Figure 10B). As revealed by XPS depth profiling of Li/g-

C_3N_4/CC, the N content decreases gradually with etching, while Li content showed an initial increase followed by a constant decrease with etching. It indicates that the surface of $g-C_3N_4$/CC after depositing Li is still $g-C_3N_4$ surface (Figure 10C). Consequently, the $g-C_3N_4$/CC scaffold enables superior cycling stability for over 1500 h with a overpotential of about 80 mV at 2 mA cm^{-2}.

Despite these great progresses, carbon-based composite LMAs still face several challenges, which may cause their failure upon repeated cycling and hinder their practical applications. First, the mechanical strengths of most carbonaceous current collectors are still far from satisfactory. This problem could be further exacerbated over charge–discharge cycles, especially at high current rates. Second, the high surface area would cause massive Li source consumption over prolonged cycling, particularly in initial several cycles. Third, the unfavorable top growth can easily occur because of the short electron transfer on the top surface of carbon-based hosts, which causes Li dendrite growth and short circuit. More research is needed to address these issues and facilitate the commercialization of carbon-based current collectors.[140]

5 | CURRENT COLLECTORS FOR SODIUM/POTASSIUM METAL ANODES

Being the members of the alkali metal group after lithium, sodium, and potassium metals have similar electrochemical properties to lithium metal. Sodium metal anode (SMA) and potassium metal anode (PMA) deliver high theoretical specific capacities of 1166 and 685 mA h g^{-1}, respectively. They also own low electrochemical potentials of -2.71 and -2.93 V (vs. SHE), respectively.[7] Moreover, sodium and potassium are much more abundant than lithium on earth, which benefits sustainable energy development (Table 1).[141] The Stokes radii of Na^+ and K^+ are smaller than that of Li^+, enabling the lower desolvation energies and higher ionic mobilities in the electrolyte.[142,143] Up to date, SMBs and PMBs have attracted intensive research attention and the developments of SMBs and PMBs have drawn on the experience of LMBs. In this section, we will summarize the strategies for current collector engineering in SMBs/PMBs, with those in which Na/K counterparts do not follow the paradigms established in LMBs highlighted above.

5.1 | Metallic current collectors

Sodium and potassium, unlike lithium, do not alloy with aluminum at low potentials.[144] Therefore, aluminum
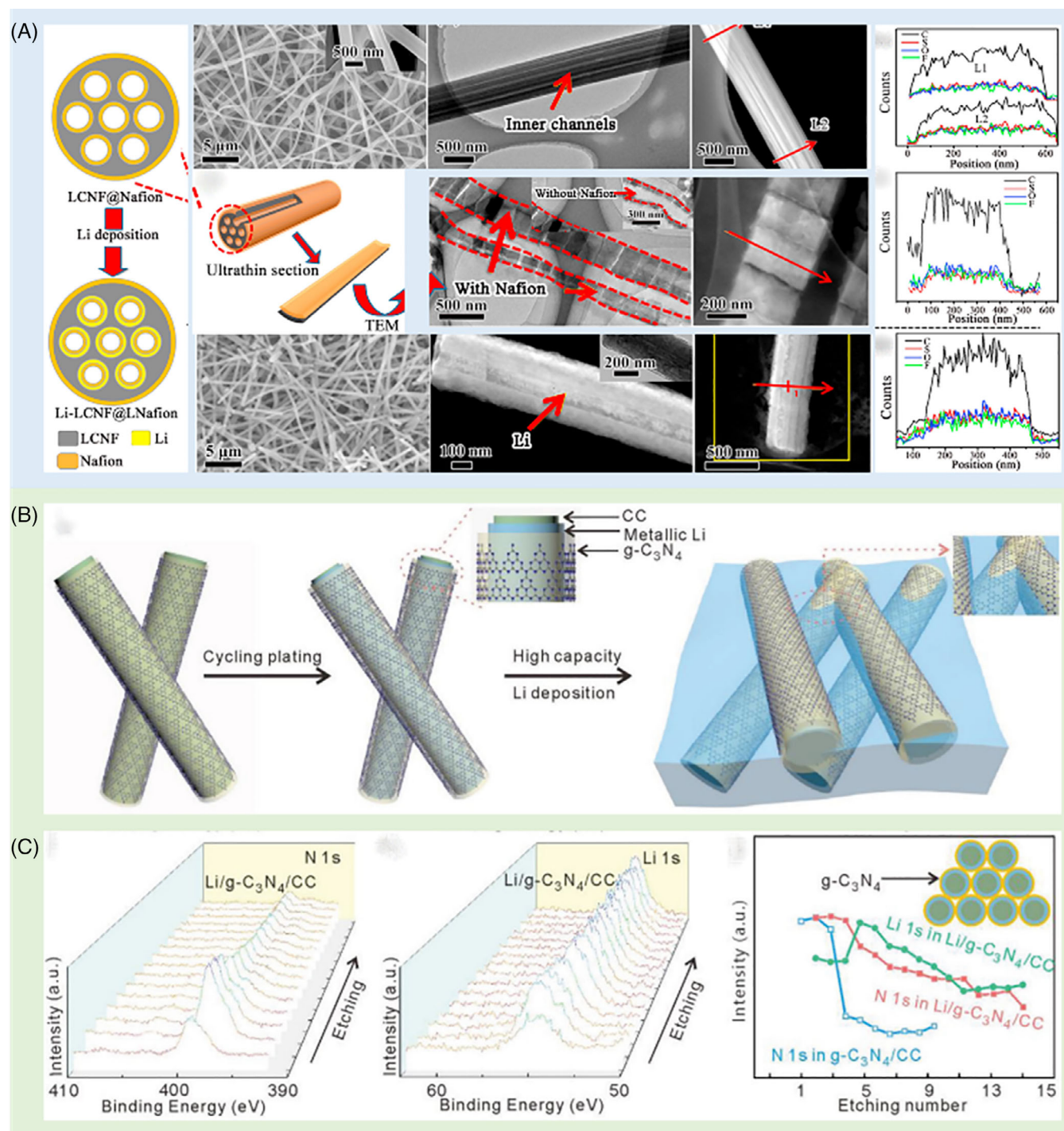
FIGURE 10 (A) Characterization of LCNF@Nafion and Li-LCNF@LNafion. Reproduced with permission: Copyright 2019, John Wiley & Sons, Inc.[139] (B) Schematic illustrations of Li deposited on the g-C_3N_4/CC scaffold. (C) XPS spectra of N 1s and Li 1s over different etching times on Li/g-C_3N_4, and depth-dependent content profiles of N in g-C_3N_4/CC, N in Li/g-C_3N_4/CC, and Li in Li/g-C_3N_4/CC. Reproduced with permission: Copyright 2019, John Wiley & Sons, Inc.[33]

foils can be used as current collectors of SMAs and PMAs. Aluminum foils have advantages in weight and cost over copper foils. For instance, porous Al current collectors with large surface areas were reported to decrease the local current density and improve the cycling stability of Na plating/stripping.[145] In another work, Cohn and co-workers coated a nanocarbon layer on the Al current collector to decrease the energy battier of Na nucleation.[146] Very recently, Jung and co-workers prepared a Cu/Al pre-patterned current collector

TABLE 1 Comparison of physical and electrochemical properties among Li, Na, and K

		Li	Na	K
Elemental properties	Atomic number	3	11	19
	Abundance (wt%)	0.0017	2.36	2.09
	Atomic mass	6.941	22.99	39.1
	Ionic radius (Å)	0.76	1.02	1.38
	Crystal structure/Lattice parameter (Å)	bcc, $Im\bar{3}m$/3.51	bcc, $Im\bar{3}m$/4.29	bcc, $Im\bar{3}m$/5.33
Physical properties	Mass density (g cm^{-3})	0.53	0.97	0.86
	Melting temperature (°C)	181	98	64
	Shear modulus (GPa)	4.2	3.3	1.3
	Brinell hardness (MPa)	5	0.69	0.36
Electrochemical properties	Redox potential vs. SHE (V)	−3.04	−2.71	−2.93
	Theoretical gravimetric specific capacity (mA h g^{-1})	3860	1166	685
	Theoretical volumetric specific capacity (mA h cm^{-3})	2045	1131	589

(Figure 11A).[147] Based on the work of adhesion (W_{ad}) and binding energy (E_b) of Na metal and metal substrates, it can be estimated that Cu substrate has a higher Na plating tendency than Al. Therefore, Cu/Al pre-patterned current collectors realized a deterministic Na growth (Figure 11B). Na ions were firstly plated on the boundary, and then a film-like aggregate was formed in the Cu region. Benefited from this well-patterned growth, the Na plating/stripping process on the prepared current collector shows an enhanced CE of 95% over 300 cycles. Another aluminum-powder-coated aluminum foil (Al@Al) current collector was reported by Liu and co-workers (Figure 11C).[148] The powders and the foil were bonded by the metallurgical bonds through an inert atmosphere high-temperature sintering process. The special surface geometry of Al@Al facilitates a fully wetted surface by a high concentration electrolyte with a contact angle of 0°. While for a planar aluminum foil, the contact angle is 52° (Figure 11D). This complete wetting of the electrolyte on the Al@Al current collector greatly decreased the amount of nonuniform SEI clumps and metal islands during K plating/stripping cycling, achieving a high average CE of 98.9% as well as a low overpotential of 85 mV.

Note that metal substrates with certain solubility in lithium can be utilized to decrease the lithium nucleation barrier.[61] Different from many metals that show high solubility in Li metal, only the main group II metals, including Be, Mg, and Ba, can be slightly dissolved in Na metal according to the binary phase diagrams.[149] Zhu and co-workers experimentally demonstrated that those main group II metal foils also can effectively decrease the sodium nucleation overpotential.[149] Compared with Cu

and Al foils, much lower sodium nucleation overpotentials were obtained on the main group II metal foils (Figure 12A). Such decreased-sodium nucleation barriers were further reflected by the morphologies of Na nucleation. Nucleated sodium with the form of spheres or domes showed uniform size distribution on main group II metal foils, while it was nonuniform on Al and Cu foils. After a continuous deposition, the morphologies of plated sodium on the main group II metal foils were flat and compact. By contrast, obvious dendrites were produced for Al and Cu foils. In another work, Sn nanoparticles and Sb micrometer particles were anchored on Cu foil to fabricate an advanced SMA current collector.[150] During the initial stage of Na deposition, M-Na (M = Sn, Sb) alloys were formed, which increase the sodiophilicity of the current collector and promote the dendrite-free deposition of Na. Similarly, Cu_3Pt alloy owns a high affinity to K, and therefore a Cu_3Pt alloy layer was coated on Cu mesh to reduce the K nucleation overpotential and guide uniform potassium deposition.[19] Very recently, Wang and co-workers also coated a layer of Pd on the surface of Cu foam to realize stable K plating/stripping cycling at low temperature.[151]

Like the current collector engineering strategies in LMAs, surface modification on planar metal current collectors has also been proposed in SMAs and PMAs. Through tuning the surface energy, current collectors with sodiophilic, or potassiophilic surfaces were constructed to inhibit the early formation of metal dendrites. Kim and co-workers tuned the plating/stripping behavior of Na metal through monolayer graphene coating on Cu foils.[152] As shown in Figure 12B, the coated graphene monolayer promoted the homogeneity of the current
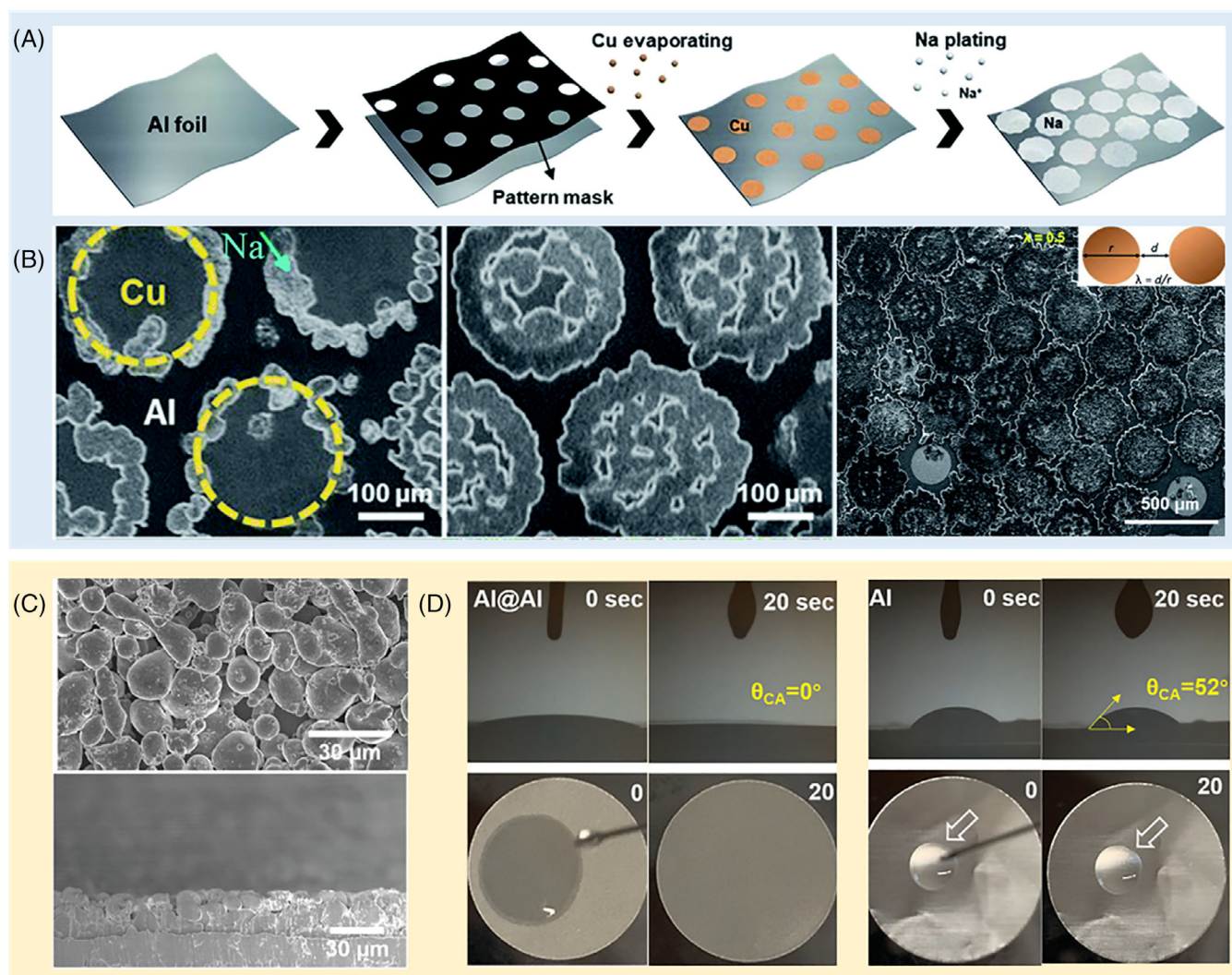
FIGURE 11 (A) Fabrication schematic of Cu/Al pre-patterned current collector. (B) SEM images of Na metal plating process and plated Na island array on a Cu/Al pre-patterned current collector. Reproduced with permission: Copyright 2012, The Royal Society of Chemistry.[147] (C) Top-down and cross-sectional SEM images of Al@Al. (D) Electrolyte wetting behavior on Al@Al versus on Al foil. Reproduced with permission: Copyright 2020, John Wiley & Sons, Inc.[148]

collector surface, which can further reduce the number of nucleation sites during the initial Na plating (Figure 12C). The homogenous surface also ensures a lower Na plating overpotential as compared with that of the bare Cu current collector (Figure 12D). Because K metal is highly active and it would spontaneously react with the electrolyte, the randomly formed SEI is inhomogeneous and easy to break during redox cycling. To minimize the reaction between K metal and electrolyte, crosslinking polyvinyl alcohol with borax (PVA-Borax) layer was coated on Cu foil proposed by Wang and co-workers.[153] Owing to the good structural stability, fast wetting process, and high K ion diffusivity, PVA-Borax functional protective layer realized a stable underneath and uniform K plating process without obvious dendrite formation (Figure 12E).

5.2 | Carbonaceous current collectors

In addition to metal current collectors, various carbonaceous current collectors were also reported in SMAs and PMAs because of their special (electro)chemical properties.[154–157] Li and co-workers compared the difference in Na dendrite formation on single-wall carbon nanotubes (SWCNT) and metal current collectors through DFT calculations.[158] The stability of Na dimers on those current collectors is a direct criterion for Na dendrite growth, because Na dimers would further aggregate into the cluster, and finally form Na dendrites. Na dimers were easily formed on metal current collector surfaces, like Cu (111) and Al (111) surfaces, while it was unstable on SWCNT surfaces, although those current collectors all have an excellent affinity with a single Na atom
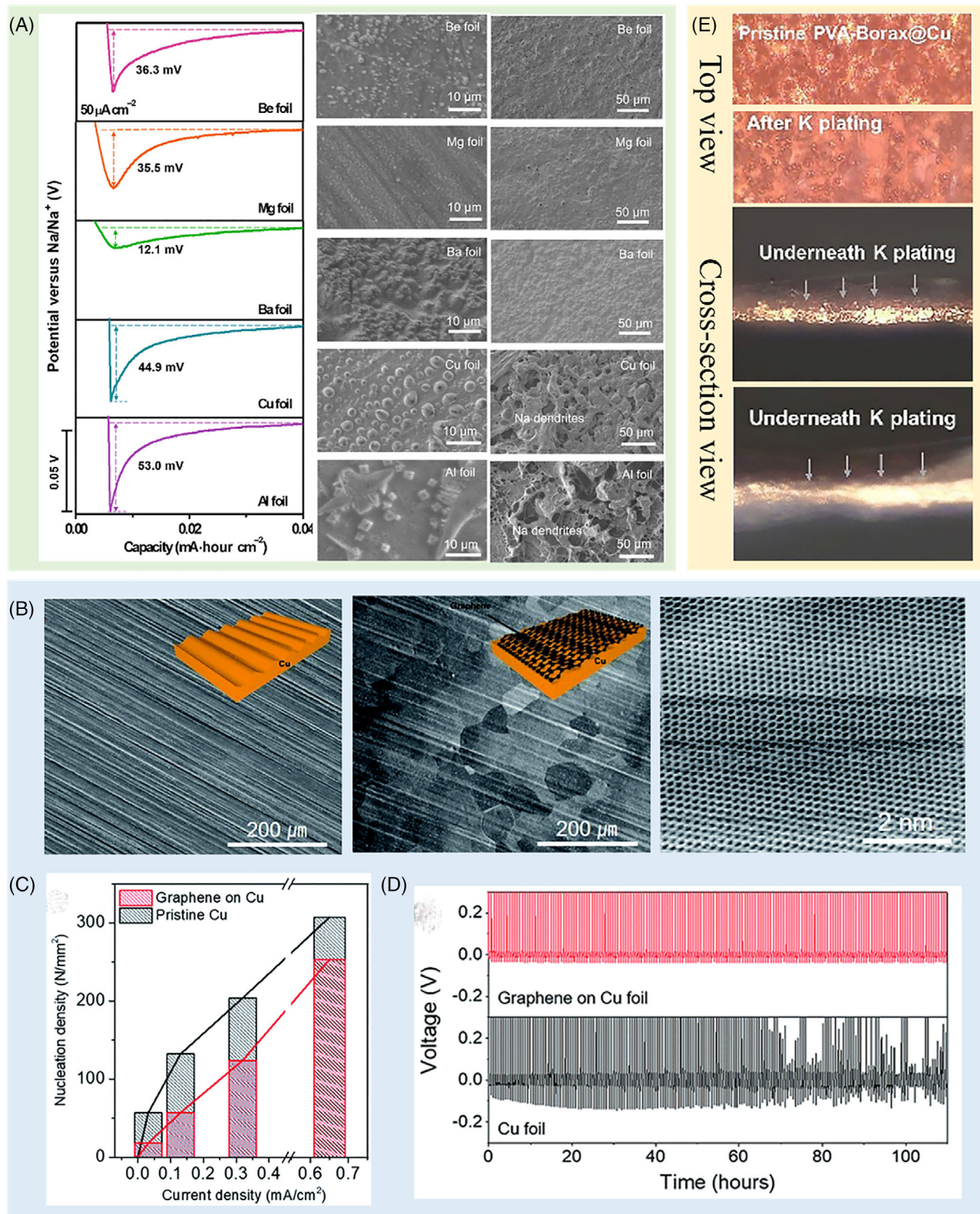
FIGURE 12 (A) Na nucleation curves on various metal foils and SEM images of deposited Na on various metal foils after depositing 0.1 mAh cm^{-2} and after depositing 0.75 mAh cm^{-2}. Reproduced with permission: Copyright 2019, the American Association for the Advancement of Science.[149] (B) Top-view SEM images of pristine Cu and graphene covered Cu current collectors, and high-resolution STM topography image of graphene covered Cu current collectors. (C) Nucleation density versus applied current of plated Na metal on pristine Cu and graphene covered Cu current collectors. (D) Chronopotentiometry plots of graphene covered Cu and pristine Cu current collectors. Reproduced with permission: Copyright 2012, The Royal Society of Chemistry.[152] (E) Top view and cross-sectional view optical microscope image of PVA-Borax@Cu and PVA-Borax@Cu after plating K. Reproduced with permission: Copyright 2021, John Wiley & Sons, Inc.[153]
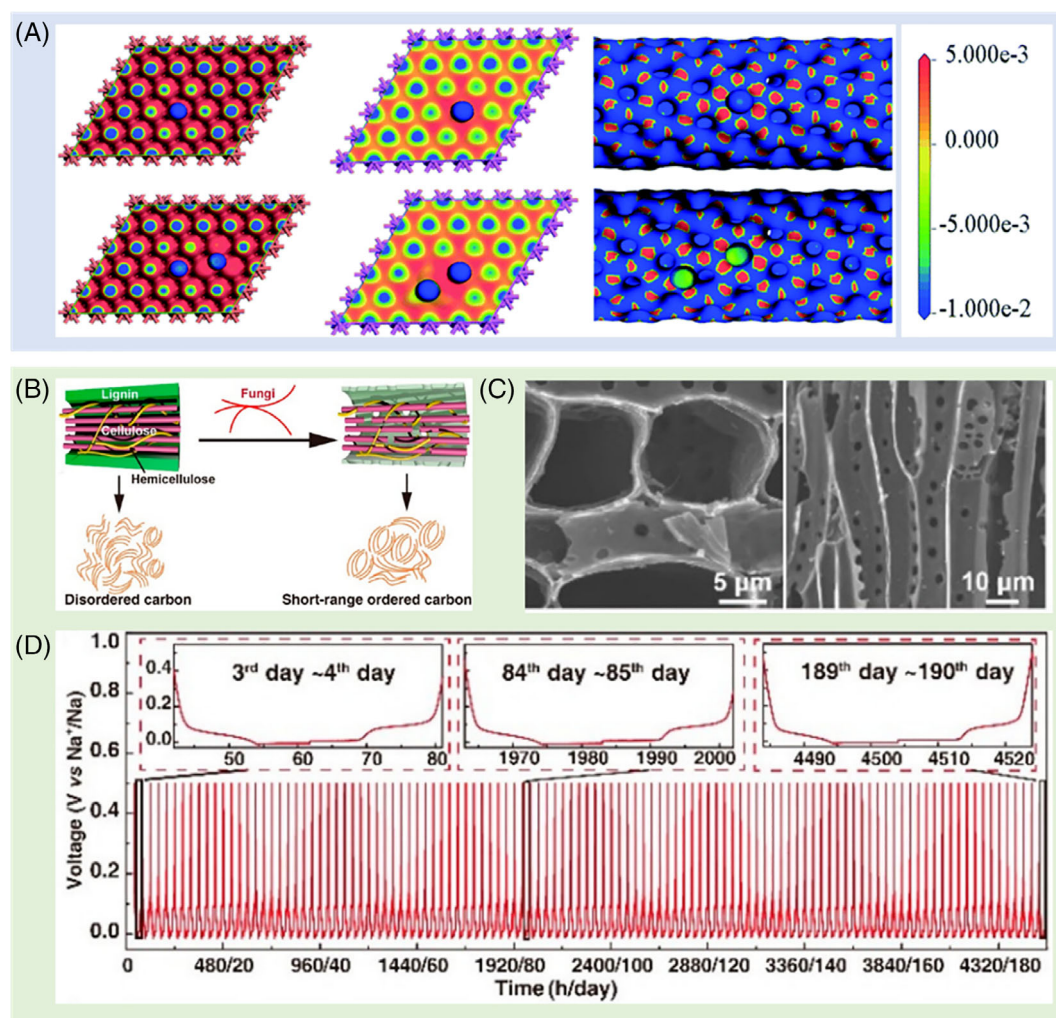
FIGURE 13 (A) The deformation electron density of single Na atoms/Na dimers adsorption on Cu (111) surface, Al (111) surface, and SWCNT surface. Reproduced with permission: Copyright 2020, The Royal Society of Chemistry.[158] (B) Schematic illustration of the fungi-assisted synthesis. (C) Top and cross-section view SEM images of the fungus-treated basswood carbon. (D) Galvanostatic discharge and charge profiles of the fungus-treated basswood carbon at 0.5 mA cm^{-2} with a capacity of 10 mAh cm^{-2}. Reproduced with permission: Copyright 2021, American Chemical Society[18]

(Figure 13A). Because of its excellent electron transfer ability and stable electronic configuration, evenly distributed Na adatoms are more favorable on the SWCNT surface, thus inhibiting the growth of dendrites. The oxygen-functionalized method was further reported to improve the sodiophilicity of CNT.[159] Yang and co-worker prepared a nitrogen-anchored Zn single atoms doped carbon cloth to adjust the uniform Na nucleation through the homogenously dispersed single Zn atoms.[160] Similarly, oxygen-containing carbonized coconut framework,[161] Au nanoparticles-modified carbon foam,[162] and Co nanoparticles embedded carbon rhombic dodecahedron[163] have been demonstrated to effectively improve the sodiophilicity of carbonaceous host and realize a stable Na plating/stripping process.

The lattice parameters of Na and K in the typical body-centered cubic crystal structure are 4.29 and 5.33 Å, much larger than that of Li (3.51 Å). As a result, there would be significantly more volume changes during

Na/K plating/stripping, which requires special consideration in carbon host design.[157,164] A fungi-assisted synthesis of highly graphitized basswood-derived carbon was proposed to serve as a Na host by Wang and co-workers in 2021.[18] The hydroxyl radicals, produced by the fungi utilizing Fenton reaction chemistry, can selectively etch the lignin skeleton through the oxidation reaction (Figure 13B). Then it was converted to a short-range ordered graphitic electrode by carbonization without any further activation process. The vertically oriented channel structure carbon skeleton can effectively limit the volume changes during Na plating/stripping cycles (Figure 13C). Thus, the prepared carbon electrode shows an average CE of 99.5% at 0.5 mA cm^{-2} with a high areal capacity of 10 mAh cm^{-2} for more than 4500 h (>190 days) (Figure 13D). Mubarak and co-workers prepared a hierarchically porous skeletal carbon nanofiber host in 2022 through electrospinning of renewable lignin
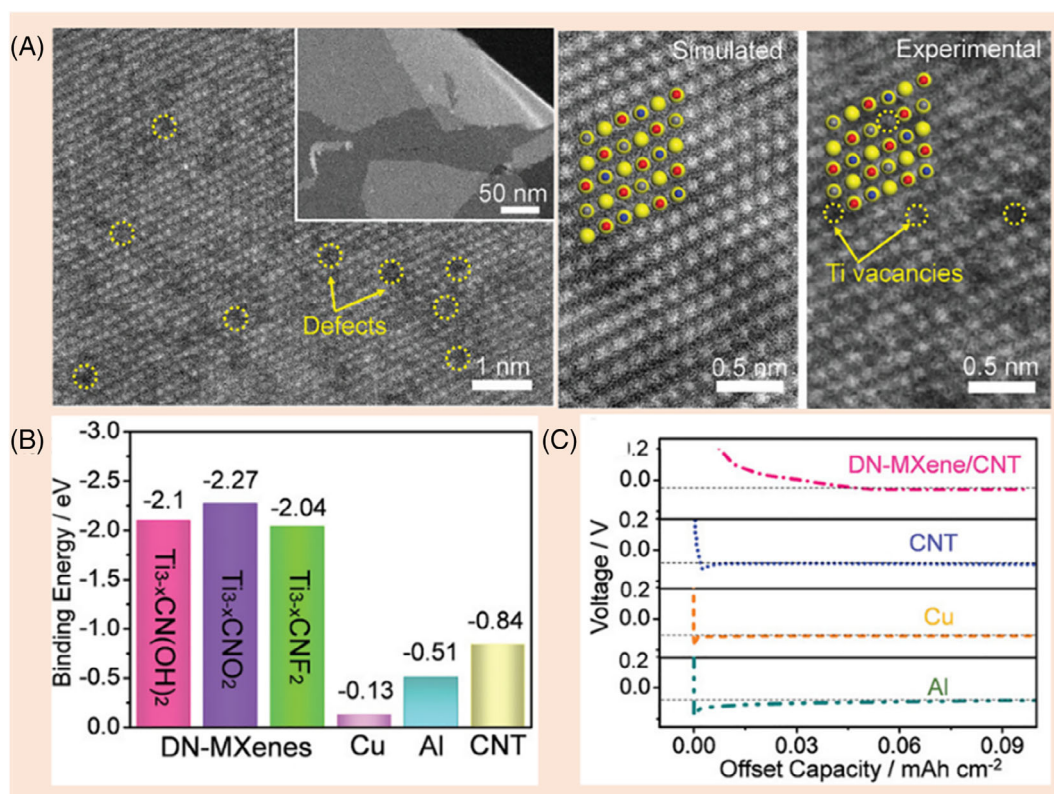
FIGURE 14 (A) High-magnification HAADF-STEM images of DN-MXene sheets, and the simulated as well as corresponding experimental atomic-resolution HAADF-STEM images of the DN-MXene sheets. (B) The calculated binding energies between K atoms and different substrates by DFT calculations. (C) The voltage profiles of K nucleation on different substrates. Reproduced with permission: Copyright 2019, John Wiley & Sons, Inc.[167]

biopolymer.[165] The defect-rich aromatic structure formed a resilient, F-rich SEI layer for Na homogenously depositing throughout the entire host structure. Qiao and co-workers revealed that highly potassiophilic amine groups significantly enhance the wettability of potassium to carbon scaffolds, which increases nucleation sites, decreases the local current density, and facilitates nondendritic Na deposition.[166]

Since the discovery of MXenes in 2011, they have been widely used in alkali metal batteries to make use of their adjustable electronic structure and physicochemical properties. The wide layer spacing of MXenes could be embedded with ions of large sizes, such as Na^+ and K^+, and ensure low migration resistances. Moreover, their composites with carbon can effectively improve the alkali metal affinity of carbonaceous host materials. Tang and co-workers fabricated a titanium-deficient nitrogen-containing MXene (DN-MXene)/CNT scaffold.[167] Abundant Ti vacancies were formed because of the slight lattice distortion when carbon atoms in the MXene structure were substituted by nitrogen, as shown in the simulated and experimental high angle annular dark-field scanning transmission electron microscopy (HAADF-STEM) images (Figure 14A). According to the DFT calculations, the substitution of carbon by nitrogen in the

N-containing MXene layer can significantly enhance the interaction with K atoms. The introduction of Ti vacancies can further increase the binding energies of K^+ ions (Figure 14B). Because of the highly potassiophilic feature of the DN-MXene sheets in the scaffold, the electrode shows a significantly decreased K nucleation overpotential (Figure 14C). Moreover, the potassiophilic MXene sheets act as "seed points" to guide the K nucleation, avoiding the K plating outside of the scaffold. Similarly, MXene-coated carbon cloth hosts,[168] and fibrous hydroxylated MXene/carbon nanotube composites,[169] were demonstrated to improve the sodiophilicity of the skeleton and promote a dendrite-free sodium plating.

6 | SUMMARY AND PERSPECTIVES

Alkali metals have attracted increasing research attention as promising alternative anodes for next-generation batteries. Current collectors are electric bridging components that collect electrical current generated at the battery electrodes and thus are regarded as the key elements in a working battery cell. An appropriate design of current collector in alkali metal batteries could enable

smooth electron conduction, lowered localized current density, and homogenized distribution of alkali metal ion flux, thus leading to uniform alkali metal nucleation and growth without any dendrite formation. Normally, the commercially available planar metal current collectors in lithium-ion batteries cannot satisfy the above requirements. A variety of current collector engineering strategies have been proposed in the past decade as have been reviewed in this article.

Metallic current collectors have high electronic conductivity, good (electro)chemical stability, easiness of 3D architecture fabrication, and functional surface modification. 3D current collectors could serve as high-surface-area alkali metal hosts to mitigate volume changes, decrease the local current density and thus promote the even distribution of Li^+ flux. However, the mechanical strengths of 3D metallic current collectors need to be further improved, and the costs for large-scale fabrication are still high. Modification on the current collector surface by functional materials could effectively drop the Li nucleation barrier and facilitate homogeneous nucleation. Alloying metals and metal compounds are typical modification materials featuring excellent affinity to lithium. Carbon modification could effectively induce uniform Li nucleation and adjust Li^+ flux thus inhibiting Li dendrite growth. Organic materials own (electro)chemical inertness, good mechanical properties, and generally lithiophilic features, thus enabling effective inhibition of Li dendrite growth and the homogenous Li deposition. Besides metal-, carbon-, and organic-based decorations, novel modification materials, such as g-C_3N_4, h-BN, and garnet-type materials can also afford the current collectors with attractive functionalities to extend the cycle life of lithium metal batteries. But these advantages would gradually disappear under practical testing conditions because of the rapid accumulation of dead Li, which blocks the Li^+ diffusion channels to lithiophilic sites.

Carbonaceous current collectors are promising alternative current collectors in alkali anode batteries because of their (electro)chemical stability, lightweight, great variety of structures, and diversified preparation methods. Carbon materials such as carbon fibers and carbon nanotubes have been employed to build 3D architectures with various heteroatoms employed to improve the lithiophilicity of carbon matrices. Metals and metal compounds have also been utilized as decoration material on carbon hosts to boost the affinity of current collectors with Li^+ ions. However, carbonaceous current collectors still exist problems including relatively lower electrical conductivities than metals, unsatisfying mechanical strengths, and high surface area derived massive lithium consumption in the initial cycles.

Sodium/potassium metal batteries are promising alternatives to replace lithium metal batteries given their natural abundance, wide distribution, and low cost of Na/K, together with the imminent commercialization of sodium-ion batteries. To develop such batteries with safe and long service life, extensive research work has been conducted on the current collector engineering for lithium metal batteries, especially the 3D architectural design and functional surface modification. Most of the knowledge created for lithium metal batteries can be applied to the sodium/potassium metal batteries. However, there are some cases where Na/K counterparts do not follow the paradigms established from lithium metal batteries. The most typical example is that aluminum foils can be used as current collectors for Na/K metal anodes since Al does not alloy with Na/K. Moreover, the main group II metals such as Be, Mg, and Ba, have certain solubilities in Na metal, leading to very low sodium nucleation overpotentials. Besides, the lattice parameters of Na and K in the body-centered cubic crystal structure are much larger than that of Li. Thus, more significant volume changes need to be considered when designing functional current collectors in SMBs and PMBs.

Despite the extensive research progress achieved above, there are still many challenges to overcome in the design of advanced current collectors for alkali metal batteries as summarized below:

1. The dilemma in non-planar current collector design: high surface area corresponds to low localized current density but meanwhile results in more side reactions and consumption of alkali metal source at the electrode surface; large porosity benefits smooth mass transportation yet leads to low mass density and poor mechanical strengths.
2. The ambiguity on the understanding of the mechanism behind alkali metal nucleation and growth control by functional modification on the current collector: The knowledge we obtained on this aspect is so far very limited and it needs more in-depth investigations, especially cutting edge in-situ characterization at electrochemical interfaces.
3. The lacking of theoretical guideline in material and structure design for current collector modification: The reported work about functional modification on current collectors still follows a trial-and-error mode. The theoretical understanding with informed strategies is in demand to improve the efficiencies.
4. The demand of simple and economical synthesis processes of advanced current collectors: The present approaches are still complex and cost-expensive. The fabricated current collectors are not compatible with the current roll-to-roll production procedure in the battery industry.

More efforts that could promote the development of novel current collectors in alkali metal batteries toward

practical applications can be made in the following directions:

1. Developing efficient simulation methods to screen and optimize the metallic, carbonaceous, and organic modification materials, using methods such as high-throughput and virtual screening to identify lead systems and estimate the critical structure–property limits.
2. Exploiting advanced characterization techniques for in-situ monitoring alkali metal deposition at electrochemical interfaces, therefore clarifying the mechanism of alkali metal nucleation and growth control by functional modification on the current collector surface.
3. Exploring facile and low-cost current collector fabrication procedures; enhancing the mechanical properties of as-fabricated current collectors to be more compatible with the present commercial roll-to-roll production procedures.
4. Formulating practical pouch-cell test in alkali metal batteries (areal capacity $\geq$2.0 mAh cm^{-2} and areal current density $\geq$4.0 mA cm^{-2}). Performing battery safety estimations in industrial standards, including storage tests at high temperature, mechanical abuse evaluation, and failure propagation measurement.

AUTHOR CONTRIBUTIONS

Liang Hu and Jiaojiao Deng contributed to conceptualization and writing the original draft; Qinghua Liang, Junxiong Wu, Bingcheng Ge and Qiang Liu assisted in reviewing; Guohua Chen and Xiaoliang Yu contributed to conceptualization, supervision, writing, reviewing and editing.

ACKNOWLEDGMENTS

CONFLICT OF INTEREST

The authors declare no conflict of interest.

ORCID

Xiaoliang Yu https://orcid.org/0000-0003-3431-3868

REFERENCES

1. Yoshino A. The birth of the lithium-ion battery. *Angew Chem Int Ed*. 2012;51(24):5798-5800. doi:10.1002/anie.201105006
2. Xu M, Jakobs S, Mazzarello R, et al. Impact of pressure on the resonant bonding in chalcogenides. *J Phys Chem C*. 2017;121(45):25447-25454. doi:10.1021/acs.jpcc.7b07546
3. Armand M, Tarascon JM. Building better batteries. *Nature*. 2008;451(7179):652-657. doi:10.1038/451652a
4. Teng WM, Wu JX, Liang QH, et al. Designing advanced liquid electrolytes for alkali metal batteries: principles, progress, and perspectives. *Energy Environ Mater*. 2022. doi:10.1002/eem2.12355
5. Wu JX, Lin C, Liang QH, et al. Sodium-rich nasicon-structured cathodes for boosting the energy density and life-span of sodium-free-anode sodium metal batteries. *Info Mat*. 2022;4(4):e12288. doi:10.1002/inf2.12288
6. Rajagopalan R, Tang YG, Ji XB, Jia CK, Wang HY. Advancements and challenges in potassium ion batteries: a comprehensive review. *Adv Funct Mater*. 2020;30(12):1909486. doi:10.1002/adfm.201909486
7. Xiang JW, Yang LY, Yuan LX, et al. Alkali-metal anodes: from lab to market. *Joule*. 2019;3(10):2334-2363. doi:10.1016/j.joule.2019.07.027
8. Peled E, Menkin S. Review-SEI: past, present and future. *J Electrochem Soc*. 2017;164(7):A1703-A1719. doi:10.1149/2.1441707jes
9. Liu H, Cheng XB, Jin ZH, et al. Recent advances in understanding dendrite growth on alkali metal anodes. *Energy Chem*. 2019;1(1):100003. doi:10.1016/j.enchem.2019.100003
10. Lv C, Zhou X, Zhong L, et al. Machine learning: An advanced platform for materials development and state prediction in lithium-ion batteries. *Adv Mater*. 2022;34(25):e2101474. doi:10.1002/adma.202101474
11. Zhang JG, Xu W, Xiao J, Cao X, Liu J. Lithium metal anodes with nonaqueous electrolytes. *Chem Rev*. 2020;120(24):13312-13348. doi:10.1021/acs.chemrev.0c00275
12. Li X, Yuan LX, Liu DZ, et al. Elevated lithium ion regulation by a "natural silk" modified separator for high-performance lithium metal anode. *Adv Funct Mater*. 2021;31(18):2100537. doi:10.1002/adfm.202100537
13. Li NW, Yin YX, Yang CP, Guo YG. An artificial solid electrolyte interphase layer for stable lithium metal anodes. *Adv Mater*. 2016;28(9):1853-1858. doi:10.1002/adma.201504526
14. Chang C, Yao Y, Li R, et al. Self-healing single-ion-conductive artificial polymeric solid electrolyte interphases for stable lithium metal anodes. *Nano Energy*. 2022;93:106871. doi:10.1016/j.nanoen.2021.106871
15. Bao CY, Wang B, Liu P, et al. Solid electrolyte interphases on sodium metal anodes. *Adv Funct Mater*. 2020;30(52):2004891. doi:10.1002/adfm.202004891
16. Ye S, Wang L, Liu F, Shi P, Yu Y. Integration of homogeneous and heterogeneous nucleation growth via 3D alloy framework for stable Na/K metal anode. *eScience*. 2021;1(1):75-82. doi:10.1016/j.esci.2021.09.003
17. Lin D, Liu Y, Cui Y. Reviving the lithium metal anode for high-energy batteries. *Nat Nanotechnol*. 2017;12(3):194-206. doi:10.1038/nnano.2017.16
18. Wang P, Zhang G, Wei XY, Liu R, Gu JJ, Cao FF. Bioselective synthesis of a porous carbon collector for high-performance sodium-metal anodes. *J Am Chem Soc*. 2021;143(9):3280-3283. doi:10.1021/jacs.0c12098
19. Wang JY, Yuan JC, Chen CH, et al. Cu₃Pt alloy-functionalized Cu mesh as current collector for dendritic-free anodes of

potassium metal batteries. *Nano Energy*. 2020;75:104914. doi: 10.1016/j.nanoen.2020.104914

20. An YL, Fei HF, Zeng GF, et al. Vacuum distillation derived 3D porous current collector for stable lithium-metal batteries. *Nano Energy*. 2018;47:503-511. doi:10.1016/j.nanoen.2018.03.036

21. Li ZY, Zhang HR, Sun XL, Yang Y. Mitigating interfacial instability in polymer electrolyte-based solid-state lithium metal batteries with 4 V cathodes. *ACS Energy Lett*. 2020; 5(10):3244-3253. doi:10.1021/acsenergylett.0c01465

22. Tang S, Qiu Z, Wang XY, et al. A room-temperature sodium metal anode enabled by a sodiophilic layer. *Nano Energy*. 2018;48:101-106. doi:10.1016/j.nanoen.2018.03.039

23. Wang L, Shang J, Huang Q, et al. Smoothing the sodium-metal anode with a self-regulating alloy interface for high-energy and sustainable sodium-metal batteries. *Adv Mater*. 2021;33(41):e2102802. doi:10.1002/adma.202102802

24. Jiang Y, Wang ZX, Xu CX, et al. Atomic layer deposition for improved lithiophilicity and solid electrolyte interface stability during lithium plating. *Energy Storage Mater*. 2020;28:17-26. doi:10.1016/j.ensm.2020.01.019

25. Li D, Hu H, Chen B, Lai WY. Advanced current collector materials for high-performance lithium metal anodes. *Small*. 2022;18:e2200010. doi:10.1002/smll.202200010

26. Yue Y, Liang H. 3D current collectors for lithium-ion batteries: a topical review. *Small Methods*. 2018;2(8):1800056. doi: 10.1002/smtd.201800056

27. Liu L, Yin YX, Li JY, et al. Free-standing hollow carbon fibers as high-capacity containers for stable lithium metal anodes. *Joule*. 2017;1(3):563-575. doi:10.1016/j.joule.2017.06.004

28. Zhang XQ, Chen X, Xu R, et al. Columnar lithium metal anodes. *Angew Chem Int Ed*. 2017;56(45):14207-14211. doi:10.1002/anie.201707093

29. Yang C, Yao Y, He S, Xie H, Hitz E, Hu L. Ultrafine silver nanoparticles for seeded lithium deposition toward stable lithium metal anode. *Adv Mater*. 2017;29(3):1702714. doi:10.1002/adma.201702714

30. Zheng G, Lee SW, Liang Z, et al. Interconnected hollow carbon nanospheres for stable lithium metal anodes. *Nat Nanotechnol*. 2014;9(8):618-623. doi:10.1038/nnano.2014.152

31. Zhu B, Jin Y, Hu X, et al. Poly(dimethylsiloxane) thin film as a stable interfacial layer for high-performance lithium-metal battery anodes. *Adv Mater*. 2017;29(2):1603755. doi:10.1002/adma.201603755

32. Zhang R, Chen XR, Chen X, et al. Lithiophilic sites in doped graphene guide uniform lithium nucleation for dendrite-free lithium metal anodes. *Angew Chem Int Ed*. 2017;129(27):7872-7876. doi:10.1002/anie.201702099

33. Xu Y, Li T, Wang L, Kang Y. Interlayered dendrite-free lithium plating for high-performance lithium-metal batteries. *Adv Mater*. 2019;31(29):e1901662. doi:10.1002/adma.201901662

34. Xie J, Wang J, Lee HR, et al. Engineering stable interfaces for three-dimensional lithium metal anodes. *Sci Adv*. 2018;4(7): eaat5168. doi:10.1126/sciadv.aat5168

35. Li Y, Li Y, Pei A, et al. Atomic structure of sensitive battery materials and interfaces revealed by cryo-electron microscopy. *Science*. 2017;358(6):506-510. doi:10.1126/science.aam6014

36. Jackle M, Gross A. Microscopic properties of lithium, sodium, and magnesium battery anode materials related to possible dendrite growth. *J Chem Phys*. 2014;141(1):174710. doi:10.1063/1.4901055

37. Ely DR, Garcia RE. Heterogeneous nucleation and growth of lithium electrodeposits on negative electrodes. *J Electrochem Soc*. 2013;160(4):A662-A668. doi:10.1149/1.057304jes

38. Chazalviel J. Electrochemical aspects of the generation of ramified metallic electrodeposits. *Phys Rev A*. 1990;42(12): 7355-7367. doi:10.1103/PhysRevA.42.7355

39. Han B, Zhang Z, Zou Y, et al. Poor stability of Li_2CO_3 in the solid electrolyte interphase of a lithium-metal anode revealed by cryo-electron microscopy. *Adv Mater*. 2021;33(22): e2100404. doi:10.1002/adma.202100404

40. He Y, Ren X, Xu Y, et al. Origin of lithium whisker formation and growth under stress. *Nat Nanotechnol*. 2019;14(11):1042-1047. doi:10.1038/s41565-019-0558-z

41. Hao F, Verma A, Mukherjee PP. Mechanistic insight into dendrite–SEI interactions for lithium metal electrodes. *J Mater Chem A*. 2018;6(4):19664-19671. doi:10.1039/C8TA07997H

42. Sacci RL, Dudney NJ, More KL, et al. Direct visualization of initial SEI morphology and growth kinetics during lithium deposition by in situ electrochemical transmission electron microscopy. *Chem Comm*. 2014;50(17):2104-2107. doi:10.1039/c3cc49029g

43. Yin X, Tang W, Jung ID, et al. Insights into morphological evolution and cycling behaviour of lithium metal anode under mechanical pressure. *Nano Energy*. 2018;50:659-664. doi:10.1016/j.nanoen.2018.06.003

44. Shi F, Pei A, Vailionis A, et al. Strong texturing of lithium metal in batteries. *Proc Natl Acad Sci U S A*. 2017;114(46): 12138-12143. doi:10.1073/pnas.1708224114

45. Rosso M, Gobron T, Brissot C, Chazalviel JN, Lascaud S. Onset of dendritic growth in lithium/polymer cells. *J Power Sources*. 2001;97-8:804-806. doi:10.1016/S0378-7753(01)00734-0

46. Lu YY, Tikekar M, Mohanty R, Hendrickson K, Ma L, Archer LA. Stable cycling of lithium metal batteries using high transference number electrolytes. *Adv Energy Mater*. 2015;5(9):1402073. doi:10.1002/aenm.201402073

47. Chi SS, Liu YC, Song WL, Fan LZ, Zhang Q. Prestoring lithium into stable 3D nickel foam host as dendrite-free lithium metal anode. *Adv Funct Mater*. 2017;27(2):1700348. doi:10.1002/adfm.201700348

48. Liu YC, Gao D, Xiang HF, Feng XY, Yu Y. Research progress on copper-based current collector for lithium metal batteries. *Energy Fuel*. 2021;35(1):12921-12937. doi:10.1021/acs.energyfuels.1c02008

49. Jiao S, Zheng J, Li Q, et al. Behavior of lithium metal anodes under various capacity utilization and high current density in lithium metal batteries. *Joule*. 2018;2(1):110-124. doi:10.1016/j.joule.2017.10.007

50. Yang CP, Yin YX, Zhang SF, Li NW, Guo YG. Accommodating lithium into 3D current collectors with a submicron skeleton towards long-life lithium metal anodes. *Nat Commun*. 2015;6(1):8058. doi:10.1038/ncomms9058

51. Yun Q, He YB, Lv W, et al. Chemical dealloying derived 3D porous current collector for Li metal anodes. *Adv Mater*. 2016; 28(32):6932-6939. doi:10.1002/adma.201601409

52. Wang SH, Yin YX, Zuo TT, et al. Stable Li metal anodes via regulating lithium plating/stripping in vertically aligned microchannels. *Adv Mater*. 2017;29(40):1703729. doi:10.1002/adma.201703729

53. Lin HN, Zhang ZW, Wang YD, Zhang XL, Tie ZX, Jin Z. Template-sacrificed hot fusion construction and nanoseed modification of 3D porous copper nanoscaffold host for stable-cycling lithium metal anodes. *Adv Funct Mater*. 2021;31(30):2102735. doi:10.1002/adfm.202102735

54. Tuan NT, Park J, Lee J, Gwak J, Lee D. Synthesis of nanoporous Cu films by dealloying of electrochemically deposited cu–Zn alloy films. *Corros Sci*. 2014;80:7-11. doi:10.1016/j.corsci.2013.11.043

55. Zhao H, Lei DN, He YB, et al. Compact 3D copper with uniform porous structure derived by electrochemical dealloying as dendrite-free lithium metal anode current collector. *Adv Energy Mater*. 2018;8(19):1800266. doi:10.1002/aenm.201800266

56. Shi YJ, Wang ZB, Gao H, et al. A self-supported, three-dimensional porous copper film as a current collector for advanced lithium metal batteries. *J Mater Chem A*. 2019;7(3):1092-1098. doi:10.1039/C8TA09384A

57. Chen J, Zhao J, Lei L, et al. Dynamic intelligent Cu current collectors for ultrastable lithium metal anodes. *Nano Lett*. 2020;20(5):3403-3410. doi:10.1021/acs.nanolett.0c00316

58. Chen KH, Sanchez AJ, Kazyak E, Davis AL, Dasgupta NP. Synergistic effect of 3D current collectors and ALD surface modification for high Coulombic efficiency lithium metal anodes. *Adv Energy Mater*. 2019;9(4):1802534. doi:10.1002/aenm.201802534

59. Wang Y, Wang Z, Lei D, et al. Spherical Li deposited inside 3D Cu skeleton as anode with ultrastable performance. *ACS Appl Energy Mater*. 2018;10(24):20244-20249. doi:10.1021/acsami.8b04881

60. Lu LL, Ge J, Yang JN, et al. Free-standing copper nanowire network current collector for improving lithium anode performance. *Nano Lett*. 2016;16(7):4431-4437. doi:10.1021/acs.nanolett.6b01581

61. Yan K, Lu ZD, Lee HW, et al. Selective deposition and stable encapsulation of lithium through heterogeneous seeded growth. *Nat Energy*. 2016;1(3):1-8. doi:10.1038/nenergy.2016.10

62. Ye H, Zheng ZJ, Yao HR, et al. Guiding uniform Li plating/stripping through lithium-aluminum alloying medium for long-life Li metal batteries. *Angew Chem Int Ed*. 2019;58(4):1094-1099. doi:10.1002/anie.201811955

63. Cui S, Zhai P, Yang W, et al. Large-scale modification of commercial copper foil with lithiophilic metal layer for Li metal battery. *Small*. 2020;16(5):e1905620. doi:10.1002/smll.201905620

64. Wang JR, Wang MM, Chen F, et al. In-situ construction of lithiophilic interphase in vertical micro-channels of 3D copper current collector for high performance lithium-metal batteries. *Energy Storage Mater*. 2021;34:22-27. doi:10.1016/j.ensm.2020.09.002

65. Lin LD, Suo LM, Hu YS, Li H, Huang XJ, Chen LQ. Epitaxial induced plating current-collector lasting lifespan of anode-free lithium metal battery. *Adv Energy Mater*. 2021;11(9):2003709. doi:10.1002/aenm.202003709

66. Zhang C, Lyu R, Lv W, et al. A lightweight 3D Cu nanowire network with phosphidation gradient as current collector for high-density nucleation and stable deposition of lithium. *Adv Mater*. 2019;31(48):e1904991. doi:10.1002/adma.201904991

67. Zhang D, Dai A, Wu M, et al. Lithiophilic 3D porous CuZn current collector for stable lithium metal batteries. *ACS Energy Lett*. 2019;5(1):180-186. doi:10.1021/acsenergylett.9b01987

68. Zhang Q, Luan JY, Tang YG, Ji XB, Wang SY, Wang HY. A facile annealing strategy for achieving in situ controllable Cu_2O nanoparticle decorated copper foil as a current collector for stable lithium metal anodes. *J Mater Chem A*. 2018;6(38):18444-18448. doi:10.1039/C8TA07612J

69. Zhang C, Lv W, Zhou GM, et al. Vertically aligned lithiophilic CuO nanosheets on a Cu collector to stabilize lithium deposition for lithium metal batteries. *Adv Energy Mater*. 2018;8(21):1703404. doi:10.1002/aenm.201703404

70. Luan J, Zhang Q, Yuan H, et al. Plasma-strengthened lithiophilicity of copper oxide nanosheet-decorated Cu foil for stable lithium metal anode. *Adv Sci*. 2019;6(20):1901433. doi:10.1002/advs.201901433

71. Qin KQ, Holguin K, Mohammadiroudbari M, et al. Strategies in structure and electrolyte design for high-performance lithium metal batteries. *Adv Funct Mater*. 2021;31(15):2009694. doi:10.1002/adfm.202009694

72. Zhang RH, Li Y, Qiao L, et al. Atomic layer deposition assisted superassembly of ultrathin ZnO layer decorated hierarchical Cu foam for stable lithium metal anode. *Energy Storage Mater*. 2021;37:123-134. doi:10.1016/j.ensm.2021.01.028

73. Huang S, Zhang W, Ming H, Cao G, Fan LZ, Zhang H. Chemical energy release driven lithiophilic layer on 1 m^2 commercial brass mesh toward highly stable lithium metal batteries. *Nano Lett*. 2019;19(3):1832-1837. doi:10.1021/acs.nanolett.8b04919

74. Zhai PB, Wei Y, Xiao J, et al. In situ generation of artificial solid-electrolyte interphases on 3D conducting scaffolds for high-performance lithium-metal anodes. *Adv Energy Mater*. 2020;10(8):1903339. doi:10.1002/aenm.201903339

75. Zhu RJ, Zhu CY, Sheng N, Rao ZH, Aoki Y, Habazaki H. A widely applicable strategy to convert fabrics into lithiophilic textile current collector for dendrite-free and high-rate capable lithium metal anode. *Chem Eng J*. 2020;388:124256. doi:10.1016/j.cej.2020.124256

76. Lei M, Wang JG, Ren L, et al. Highly lithiophilic cobalt nitride nanobrush as a stable host for high-performance lithium metal anodes. *ACS Appl Energy Mater*. 2019;11(34):30992-30998. doi:10.1021/acsami.9b09975

77. Tan J, Matz J, Dong P, Shen JF, Ye MX. A growing appreciation for the role of LiF in the solid electrolyte interphase. *Adv Energy Mater*. 2021;11(16):2100046. doi:10.1002/aenm.202100046

78. Huang G, Chen S, Guo P, et al. In situ constructing lithiophilic NiF_x nanosheets on Ni foam current collector for stable lithium metal anode via a succinct fluorination strategy. *Chem Eng J*. 2020;395:125122. doi:10.1016/j.cej.2020.125122

79. Liu YY, Tzeng YK, Lin DC, et al. An ultrastrong double-layer nanodiamond interface for stable lithium metal anodes. *Joule*. 2018;2(8):1595-1609. doi:10.1016/j.joule.2018.05.007

80. Zhang AY, Fang X, Shen CF, Liu YH, Zhou CW. A carbon nanofiber network for stable lithium metal anodes with high coulombic efficiency and long cycle life. *Nano Res*. 2016;9(11):3428-3436. doi:10.1007/s12274-016-1219-2

81. Duan H, Zhang J, Chen X, et al. Uniform nucleation of lithium in 3D current collectors via bromide intermediates for stable cycling lithium metal batteries. *J Am Chem Soc*. 2018; 140(51):18051-18057. doi:10.1021/jacs.8b10488

82. Kim MS, Ryu JH. Deepika, et al. Langmuir-Blodgett artificial solid-electrolyte interphases for practical lithium metal batteries. *Nat Energy*. 2018;3(10):889-898. doi:10.1038/s41560-018-0237-6

83. Song RS, Wang B, Xie Y, et al. A 3D conductive scaffold with lithiophilic modification for stable lithium metal batteries. *J Mater Chem A*. 2018;6(37):17967-17976. doi:10.1039/C8TA06775A

84. Yan K, Sun B, Munroe P, Wang GX. Three-dimensional pie-like current collectors for dendrite-free lithium metal anodes. *Energy Storage Mater*. 2018;11:127-133. doi:10.1016/j.ensm.2017.10.012

85. Yang GH, Chen JD, Xiao PT, Agboola PO, Shakir I, Xu YX. Graphene anchored on Cu foam as a lithiophilic 3D current collector for a stable and dendrite-free lithium metal anode. *J Mater Chem A*. 2018;6(21):9899-9905. doi:10.1039/C8TA02810A

86. Zhang R, Wen SW, Wang N, et al. N-doped graphene modified 3D porous Cu current collector toward microscale homogeneous Li deposition for Li metal anodes. *Adv Energy Mater*. 2018;8(23):1800914. doi:10.1002/aenm.201800914

87. Assegie AA, Chung CC, Tsai MC, Su WN, Chen CW, Hwang BJ. Multilayer-graphene-stabilized lithium deposition for anode-free lithium-metal batteries. *Nanoscale*. 2019;11(6): 2710-2720. doi:10.1039/C8NR06980H

88. Huang SY, Tang L, Najafabadi HS, Chen S, Ren ZF. A highly flexible semi-tubular carbon film for stable lithium metal anodes in high-performance batteries. *Nano Energy*. 2017;38: 504-509. doi:10.1016/j.nanoen.2017.06.030

89. Jin CB, Sheng OW, Luo JM, et al. 3D lithium metal embedded within lithiophilic porous matrix for stable lithium metal batteries. *Nano Energy*. 2017;37:177-186. doi:10.1016/j.nanoen.2017.05.015

90. Ye H, Xin S, Yin YX, Li JY, Guo YG, Wan LJ. Stable Li plating/stripping electrochemistry realized by a hybrid Li reservoir in spherical carbon granules with 3D conducting skeletons. *J Am Chem Soc*. 2017;139(16):5916-5922. doi:10.1021/jacs.7b01763

91. Xu ZX, Xu LY, Xu ZX, Deng ZP, Wang XL. N, O-codoped carbon nanosheet array enabling stable lithium metal anode. *Adv Funct Mater*. 2021;31(4):2102354. doi:10.1002/adfm.202102354

92. Li J, Cai Y, Wu H, et al. Polymers in lithium-ion and lithium metal batteries. *Adv Energy Mater*. 2021;11(15):2003239. doi:10.1002/aenm.202003239

93. Du Y, Gao X, Li SW, Wang L, Wang B. Recent advances in metal-organic frameworks for lithium metal anode protection. *Chin Chem Lett*. 2020;31(3):609-616. doi:10.1016/j.cclet.2019.06.013

94. Assegie AA, Cheng JH, Kuo LM, Su WN, Hwang BJ. Polyethylene oxide film coating enhances lithium cycling efficiency of an anode-free lithium-metal battery. *Nanoscale*. 2018; 10(13):6125-6138. doi:10.1039/C7NR09058G

95. Luo J, Fang CC, Wu NL. High polarity poly(vinylidene difluoride) thin coating for dendrite-free and high-performance lithium metal anodes. *Adv Energy Mater*. 2018; 8(2):1701482. doi:10.1002/aenm.201701482

96. Liu W, Lin D, Pei A, Cui Y. Stabilizing lithium metal anodes by uniform Li-ion flux distribution in nanochannel confinement. *J Am Chem Soc*. 2016;138(47):15443-15450. doi:10.1021/jacs.6b08730

97. Yu ZA, Mackanic DG, Michaels W, et al. A dynamic, electrolyte-blocking, and single-ion-conductive network for stable lithium-metal anodes. *Joule*. 2019;3(11):2761-2776. doi:10.1016/j.joule.2019.07.025

98. Zou P, Wang Y, Chiang SW, Wang X, Kang F, Yang C. Directing lateral growth of lithium dendrites in micro-compartmented anode arrays for safe lithium metal batteries. *Nat Commun*. 2018;9(1):464. doi:10.1038/s41467-018-02888-8

99. Song YW, Shi P, Li BQ, et al. Covalent organic frameworks construct precise lithiophilic sites for uniform lithium deposition. *Matter*. 2021;4(1):253-264. doi:10.1016/j.matt.2020.10.014

100. Liu K, Pei A, Lee HR, et al. Lithium metal anodes with an adaptive "solid-liquid" interfacial protective layer. *J Am Chem Soc*. 2017;139(13):4815-4820. doi:10.1021/jacs.6b13314

101. Zheng GY, Wang C, Pei A, et al. High-performance lithium metal negative electrode with a soft and flowable polymer coating. *ACS Energy Lett*. 2016;1(6):1247-1255. doi:10.1021/acsenergylett.6b00456

102. Yue XY, Wang WW, Wang QC, et al. Cuprite-coated Cu foam skeleton host enabling lateral growth of lithium dendrites for advanced Li metal batteries. *Energy Storage Mater*. 2019;21: 180-189. doi:10.1016/j.ensm.2018.12.007

103. Jiang ZG, Liu TF, Yan LJ, et al. Metal-organic framework nanosheets-guided uniform lithium deposition for metallic lithium batteries. *Energy Storage Mater*. 2018;11:267-273. doi:10.1016/j.ensm.2017.11.003

104. Fan LS, Guo ZK, Zhang Y, et al. Stable artificial solid electrolyte interphase films for lithium metal anode via metal-organic frameworks cemented by polyvinyl alcohol. *J Mater Chem A*. 2020;8(1):251-258. doi:10.1039/C9TA10405D

105. Zhao J, Yuan HY, Wang GL, et al. Stabilization of lithium metal anodes by conductive metal-organic framework architectures. *J Mater Chem A*. 2021;9(20):12099-12108. doi:10.1039/D1TA01568K

106. Qian J, Li Y, Zhang ML, et al. Protecting lithium/sodium metal anode with metal-organic framework based compact and robust shield. *Nano Energy*. 2019;60:866-874. doi:10.1016/j.nanoen.2019.04.030

107. Xu Y, Zhou Y, Li T, et al. Multifunctional covalent organic frameworks for high capacity and dendrite-free lithium metal batteries. *Energy Storage Mater*. 2020;25:334-341. doi:10.1016/j.ensm.2019.10.005

108. Zhao H, Sheng L, Wang L, Xu H, He XM. The opportunity of metal organic frameworks and covalent organic frameworks in lithium (ion) batteries and fuel cells. *Energy Storage Mater*. 2020;33:360-381. doi:10.1016/j.ensm.2020.08.028

109. Gao X, Dong Y, Li S, Zhou J, Wang L, Wang B. MOFs and COFs for batteries and supercapacitors. *Electrochem Energy Rev*. 2019;3(1):81-126. doi:10.1007/s41918-019-00055-1

110. Peng H, Raya J, Richard F, et al. Synthesis of robust MOFs@-COFs porous hybrid materials via an aza-diels-alder reaction: towards high-performance supercapacitor materials. *Angew*

Chem Int Ed. 2020;59(44):19602-19609. doi:10.1002/anie.202008408

111. Zhai P, Wang T, Jiang H, et al. 3D artificial solid-electrolyte interphase for lithium metal anodes enabled by insulator-metal-insulator layered heterostructures. *Adv Mater*. 2021;33(13):e2006247. doi:10.1002/adma.202006247

112. Lu ZY, Liang QH, Wang B, et al. Graphitic carbon nitride induced micro-electric field for dendrite-free lithium metal anodes. *Adv Energy Mater*. 2019;9(7):1803186. doi:10.1002/aenm.201803186

113. Xie J, Liao L, Gong Y, et al. Stitching h-BN by atomic layer deposition of LiF as a stable interface for lithium metal anode. *Sci Adv*. 2017;3(11):eaao3170. doi:10.1126/sciadv.aao3170

114. Yan K, Lee HW, Gao T, et al. Ultrathin two-dimensional atomic crystals as stable interfacial layer for improvement of lithium metal anode. *Nano Lett*. 2014;14(10):6016-6022. doi:10.1021/nl503125u

115. Li P, Dong X, Li C, et al. Anchoring an artificial solid-electrolyte interphase layer on a 3D current collector for high-performance lithium anodes. *Angew Chem Int Ed*. 2019;58(7):2093-2097. doi:10.1002/anie.201813905

116. Li N, Wei W, Xie K, et al. Suppressing dendritic lithium formation using porous media in lithium metal-based batteries. *Nano Lett*. 2018;18(3):2067-2073. doi:10.1021/acs.nanolett.8b00183

117. Chen W, Salvatierra RV, Ren M, Chen J, Stanford MG, Tour JM. Laser-induced silicon oxide for anode-free lithium metal batteries. *Adv Mater*. 2020;32(33):e2002850. doi:10.1002/adma.202002850

118. Kim YJ, Kwon SH, Noh H, et al. Facet selectivity of Cu current collector for Li electrodeposition. *Energy Stor Mater*. 2019;19:154-162. doi:10.1016/j.ensm.2019.02.011

119. Gu Y, Xu HY, Zhang XG, et al. Lithiophilic faceted Cu(100) surfaces: high utilization of host surface and cavities for lithium metal anodes. *Angew Chem Int Ed*. 2019;58(10):3092-3096. doi:10.1002/anie.201812523

120. Fu A, Wang CZ, Peng J, et al. Lithiophilic and antioxidative copper current collectors for highly stable lithium metal batteries. *Adv Funct Mater*. 2021;31(15):2009805. doi:10.1002/adfm.202009805

121. Wu JX, Qin XY, Miao C, et al. A honeycomb-cobweb inspired hierarchical core-shell structure design for electrospun silicon/carbon fibers as lithium-ion battery anodes. *Carbon*. 2016;98:582-591. doi:10.1016/j.carbon.2015.11.048

122. Yang G, Li Y, Tong Y, et al. Lithium plating and stripping on carbon nanotube sponge. *Nano Lett*. 2019;19(1):494-499. doi:10.1021/acs.nanolett.8b04376

123. Wang TS, Zhai PB, Legut D, et al. S-doped graphene-regional nucleation mechanism for dendrite-free lithium metal anodes. *Adv Energy Mater*. 2019;9(24):1804000. doi:10.1002/aenm.201804000

124. Zhai PB, Wang TS, Yang WW, et al. Uniform lithium deposition assisted by single-atom doping toward high-performance lithium metal anodes. *Adv Energy Mater*. 2019;9(18):1804019. doi:10.1002/aenm.201804019

125. Liu L, Yin YX, Li JY, Wang SH, Guo YG, Wan LJ. Uniform lithium nucleation/growth induced by lightweight nitrogen-doped graphitic carbon foams for high-performance lithium metal anodes. *Adv Mater*. 2018;30(10):1706216. doi:10.1002/adma.201706216

126. Xiang JW, Yuan LX, Shen Y, et al. Improved rechargeability of lithium metal anode via controlling lithium-ion flux. *Adv Energy Mater*. 2018;8(36):1802352. doi:10.1002/aenm.201802352

127. Hong B, Fan HL, Cheng XB, et al. Spatially uniform deposition of lithium metal in 3D Janus hosts. *Energy Storage Mater*. 2019;16:259-266. doi:10.1016/j.ensm.2018.04.032

128. Chen K, Pathak R, Gurung A, et al. A copper-clad lithiophilic current collector for dendrite-free lithium metal anodes. *J Mater Chem A*. 2020;8(4):1911-1919. doi:10.1039/C9TA11237E

129. Chen C, Guan J, Li NW, et al. Lotus-root-like carbon fibers embedded with Ni-co nanoparticles for dendrite-free lithium metal anodes. *Adv Mater*. 2021;33(24):e2100608. doi:10.1002/adma.202100608

130. Fang Y, Zhang SL, Wu ZP, Luan D, Lou XWD. A highly stable lithium metal anode enabled by Ag nanoparticle-embedded nitrogen-doped carbon macroporous fibers. *Sci Adv*. 2021;7(21):eabg3626. doi:10.1126/sciadv.abg3626

131. Kim BG, Kang DW, Park G, Park SH, Lee SM, Choi JW. Electrospun Li-confinable hollow carbon fibers for highly stable Li-metal batteries. *Chem Eng J*. 2021;422:130017. doi:10.1016/j.cej.2021.130017

132. Zhang Y, Liu BY, Hitz E, et al. A carbon-based 3D current collector with surface protection for Li metal anode. *Nano Res*. 2017;10(4):1356-1365. doi:10.1007/s12274-017-1461-2

133. Deng W, Zhu WH, Zhou XF, Liu ZP. Graphene nested porous carbon current collector for lithium metal anode with ultra-high areal capacity. *Energy Storage Mater*. 2018;15:266-273. doi:10.1016/j.ensm.2018.05.005

134. Tang LS, Zhang R, Zhang XY, et al. ZnO nanoconfined 3D porous carbon composite microspheres to stabilize lithium nucleation/growth for high-performance lithium metal anodes. *J Mater Chem A*. 2019;7(33):19442-19452. doi:10.1039/C9TA06401J

135. Lin K, Qin XY, Liu M, et al. Ultrafine titanium nitride sheath decorated carbon nanofiber network enabling stable lithium metal anodes. *Adv Funct Mater*. 2019;29(46):1903229. doi:10.1002/adfm.201903229

136. Liu H, Chen X, Cheng XB, et al. Uniform lithium nucleation guided by atomically dispersed lithiophilic CoN_x sites for safe lithium metal batteries. *Small Methods*. 2019;3(9):1800354. doi:10.1002/smtd.201800354

137. Luo L, Li J, Yaghoobnejad Asl H, Manthiram A. A 3D lithiophilic Mo_2N-modified carbon nanofiber architecture for dendrite-free lithium-metal anodes in a full cell. *Adv Mater*. 2019;31(48):e1904537. doi:10.1002/adma.201904537

138. Gao CH, Hong B, Sun KN, et al. Self-suppression of lithium dendrite with aluminum nitride nanoflake additive in 3D carbon paper for lithium metal batteries. *Energ Technol*. 2020;8(7):1901463. doi:10.1002/ente.201901463

139. Xiang JW, Zhao Y, Yuan LX, et al. A strategy of selective and dendrite-free lithium deposition for lithium batteries. *Nano Energy*. 2017;42:262-268. doi:10.1016/j.nanoen.2017.10.065

140. Yan XL, Lin L, Chen QL, et al. Multifunctional roles of carbon-based hosts for Li-metal anodes: a review. *Carbon Energy*. 2021;3(2):303-329. doi:10.1002/cey2.95

141. Larcher D, Tarascon JM. Towards greener and more sustainable batteries for electrical energy storage. *Nat Chem*. 2015;7(1):19-29. doi:10.1038/nchem.2085

142. Matsuda Y, Nakashima H, Morita M, Takasu Y. Behavior of some ions in mixed organic electrolytes of high-energy density batteries. *J Electrochem Soc*. 1981;128(12):2552-2556. doi:10.1149/1.2127289

143. Kubota K, Dahbi M, Hosaka T, Kumakura S, Komaba S. Towards K-ion and Na-ion batteries as "beyond Li-ion". *Chem Rec*. 2018;18(4):459-479. doi:10.1002/tcr.201700057

144. Wang H, Yu DD, Kuang CW, et al. Alkali metal anodes for rechargeable batteries. *Chem*. 2019;5(2):313-338. doi:10.1016/j.chempr.2018.11.005

145. Liu S, Tang S, Zhang X, Wang A, Yang QH, Luo J. Porous Al current collector for dendrite-free Na metal anodes. *Nano Lett*. 2017;17(9):5862-5868. doi:10.1021/acs.nanolett.7b03185

146. Cohn AP, Muralidharan N, Carter R, Share K, Pint CL. Anode-free sodium battery through in situ plating of sodium metal. *Nano Lett*. 2017;17(2):1296-1301. doi:10.1021/acs.nanolett.6b05174

147. Jung J, Hwang DY, Kristanto I, Kwak SK, Kang SJ. Deterministic growth of a sodium metal anode on a pre-patterned current collector for highly rechargeable seawater batteries. *J Mater Chem A*. 2019;7(16):9773-9781. doi:10.1039/C9TA01718F

148. Liu P, Wang Y, Hao H, et al. Stable potassium metal anodes with an all-aluminum current collector through improved electrolyte wetting. *Adv Mater*. 2020;32(49):e2002908. doi:10.1002/adma.202002908

149. Zhu M, Li S, Li B, Gong Y, Du Z, Yang S. Homogeneous guiding deposition of sodium through main group II metals toward dendrite-free sodium anodes. *Sci Adv*. 2019;5(4):eaau6264. doi:10.1126/sciadv.aau6264

150. Tang S, Zhang YY, Zhang XG, et al. Stable Na plating and stripping electrochemistry promoted by in situ construction of an alloy-based sodiophilic interphase. *Adv Mater*. 2019;31(16):e1807495. doi:10.1002/adma.201807495

151. Wang JY, Yan W, Zhang JJ. High area capacity and dendrite-free anode constructed by highly potassiophilic Pd/Cu current collector for low-temperature potassium metal battery. *Nano Energy*. 2022;96:107131. doi:10.1016/j.nanoen.2022.107131

152. Kim DH, Choi H, Hwang DY, et al. Reliable seawater battery anode: controlled sodium nucleationviadeactivation of the current collector surface. *J Mater Chem A*. 2018;6(40):19672-19680. doi:10.1039/C8TA07610C

153. Wang S, Yan Y, Xiong D, et al. Towards dendrite-free potassium-metal batteries: rational design of a multifunctional 3D polyvinyl alcohol-borax layer. *Angew Chem Int Ed*. 2021;60(47):25122-25127. doi:10.1002/anie.202111753

154. Chi SS, Qi XG, Hu YS, Fan LZ. 3D flexible carbon felt host for highly stable sodium metal anodes. *Adv Energy Mater*. 2018;8(15):1702764. doi:10.1002/aenm.201702764

155. Ma CY, Xu TT, Wang Y. Advanced carbon nanostructures for future high performance sodium metal anodes. *Energy Storage Mater*. 2020;25:811-826. doi:10.1016/j.ensm.2019.09.007

156. Qiao F, Meng JS, Wang JJ, et al. Building carbon cloth-based dendrite-free potassium metal anodes for potassium metal pouch cells. *J Mater Chem A*. 2021;9(40):23046-23054. doi:10.1039/D1TA06327H

157. Zhou M, Qi W, Hu Z, et al. Highly potassiophilic carbon nanofiber paper derived from bacterial cellulose enables ultrastable dendrite-free potassium metal anodes. *ACS Appl Energy Mater*. 2021;13(15):17629-17638. doi:10.1021/acsami.1c02186

158. Li MT, Sun B, Ao ZM, An TC, Wang GX. Atomic-scale identification of influencing factors of sodium dendrite growth on different current collectors. *J Mater Chem A*. 2020;8(20):10199-10205. doi:10.1039/D0TA01853H

159. Ye L, Liao M, Zhao T, et al. A sodiophilic interphase-mediated, dendrite-free anode with ultrahigh specific capacity for sodium-metal batteries. *Angew Chem Int Ed*. 2019;58(47):17054-17060. doi:10.1002/anie.201910202

160. Yang T, Qian T, Sun Y, Zhong J, Rosei F, Yan C. Mega high utilization of sodium metal anodes enabled by single zinc atom sites. *Nano Lett*. 2019;19(11):7827-7835. doi:10.1021/acs.nanolett.9b02833

161. Li TJ, Sun JC, Gao SZ, et al. Superior sodium metal anodes enabled by sodiophilic carbonized coconut framework with 3D tubular structure. *Adv Energy Mater*. 2021;11(7):2003699. doi:10.1002/aenm.202003699

162. Wu J, Zou P, Ihsan-Ul-Haq M, et al. Sodiophilically graded gold coating on carbon skeletons for highly stable sodium metal anodes. *Small*. 2020;16(40):e2003815. doi:10.1002/smll.202003815

163. Xie YY, Hu JX, Han ZX, et al. Encapsulating sodium deposition into carbon rhombic dodecahedron guided by sodiophilic sites for dendrite-free Na metal batteries. *Energy Storage Mater*. 2020;30:1-8. doi:10.1016/j.ensm.2020.05.008

164. Liu P, Mitlin D. Emerging potassium metal anodes: perspectives on control of the electrochemical interfaces. *Acc Chem Res*. 2020;53(6):1161-1175. doi:10.1021/acs.accounts.0c00099

165. Mubarak N, Rehman F, Ihsan-Ul-Haq M, et al. Highly sodiophilic, defect-rich, lignin-derived skeletal carbon nanofiber host for sodium metal batteries. *Adv Energy Mater*. 2022;12(12):2103904. doi:10.1002/aenm.202103904

166. Meng J, Zhu H, Xiao Z, et al. Amine-wetting-enabled dendrite-free potassium metal anode. *ACS Nano*. 2022;16(5):7291-7300. doi:10.1021/acsnano.2c01432

167. Tang X, Zhou D, Li P, et al. Mxene-based dendrite-free potassium metal batteries. *Adv Mater*. 2020;32(4):e1906739. doi:10.1002/adma.201906739

168. Fang Y, Lian R, Li H, et al. Induction of planar sodium growth on MXene ($Ti_3C_2T_x$)-modified carbon cloth hosts for flexible sodium metal anodes. *ACS Nano*. 2020;14(7):8744-8753. doi:10.1021/acsnano.0c03259

169. He X, Jin S, Miao L, et al. A 3D hydroxylated mxene/carbon nanotubes composite as a scaffold for dendrite-free sodium-metal electrodes. *Angew Chem Int Ed*. 2020;59(38):16705-16711. doi:10.1002/anie.202006783

AUTHOR BIOGRAPHIES
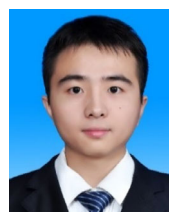
Liang Hu received his B.E. from Central South University and M.S. from University of Chinese Academy of Sciences in 2014 and 2018, respectively. Currently, he is pursuing his Ph.D. degree at The Hong Kong Polytechnic University. His research interests focus on anode-free Li/Na metal batteries.

Guohua Chen received his B.E. from Dalian University of Technology in 1984, M.E. and Ph.D. degrees from McGill University in 1989 and 1994, respectively. He joined HKUST in 1994 and was promoted as professor in 2008, and then he acted as an Endowed Otto Poon Charitable Foundation Professor at The Hong Kong Polytechnic University in 2019. He is currently a chair professor in the School of Energy and Environment of City University of Hong Kong. His main research areas include advanced electrode materials for energy storage, electrochemical technologies for energy and environmental applications, drying of high value products.

Xiaoliang Yu earned his B.S. (2011) and Ph.D. (2016) degrees in material science and engineering at Tsinghua University. After graduation, he conducted his postdoctoral research at National Institute for Material Science in Japan for three and half years. He began his career as an independent PI at The Hong Kong Polytechnic University in 2020. Now, he is a research assistant professor at the Department of Mechanical Engineering, The Hong Kong Polytechnic University. His research interests are focused on nanocarbon-based materials, interface design of composite materials, and electrochemical energy storage systems.